Integrated Master in Chemical Engineering

Functionalized Gold Nanoparticles as a versatile vehicle to delivery anticancer drugs

Master Thesis

by

Lídia Maria Carvalho Cunha

Supervisor: Manuel Álvaro Neto Coelho

Sílvia Maria de Castro Coelho

09/ 2016

“I never see what has been done;

I only see what remains to be done.”

Marie Curie

Acknowledgments

This work was financially supported by the projects POCI-01-0145-FEDER-006939 - Laboratory for Process Engineering, Environment, Biotechnology and Energy – LEPABE and NORTE-01-0145-FEDER-000005 – LEPABE-2-ECO-INNOVATION, funded by FEDER funds through COMPETE2020 - Programa Operacional Competitividade e Internacionalização (POCI) and Programa Operacional Regional do Norte (NORTE2020) and by national funds through FCT - Fundação para a Ciência e a Tecnologia; Project Reference if applicable and Scholarship Reference if applicable.

I would like to express my profound gratefulness to Professor Manuel Coelho and Silvia Castro Coelho for their scientific mentoring and advice. A special thanks to Silvia Castro Coelho for her available and knowledge, for her supervision and helpful comments, which were indispensable to accomplish my thesis.

I'm thankful to Daniela Correia, for her kindness and support as a friend.

I would like to thanks to my parents for their love and comprehension, to my brother for having the right advice at the right time. Lastly, I'm grateful to Abílio Costa for his dedication, affection and support.

Abstract

The aim of the presented research was to design and optimize gold nanoparticles (AuNPs) by different methods. The nanoparticles were synthetized with chitosan (a cationic polysaccharide) and with epigallocatechin gallate (EGCG). Also, gold nanoparticles were synthesized by Turkevitch method and functionalized with cysteamine, an antioxidant. Arabic gum (a polysaccharide used in food industry) was used as a stabilizer of AuNPs. The proposed nanosystems were conjugated/loaded with EGCG, a polyphenol that exhibits biological and pharmacological effects such as antioxidant, anticarcinogenic and anti-inflammatory properties.

Stable and small nanosystems were prepared with EGCG. The encapsulation efficiency of gold nanoparticles with EGCG is 34±8%. 60±2% and 78±1% of EGCG conjugation efficiency was obtained for gold nanoparticles prepared with chitosan and for functionalized gold nanoparticles with cysteamine of EGCG, respectively. The gold nanoparticles surface stabilized with arabic gum absorbed around 14 ± 2% of EGCG.

The antioxidant activity of the nanosystems was analysed and the conjugation/loading of gold nanoparticles with EGCG did not influence its activity.

The results demonstrated that EGCG can act as a reducing agent and, also, as a stabilizer of gold nanoparticles. The efficient preparation, conjugation and optimization of the nanosystems might lead to being used as a novel approach as drug delivery systems.

Keywords: gold nanoparticles, epigallocatechin gallate, conjugation, stabilizer, efficiency, antioxidant

Resumo

O estudo visa a síntese e otimização de sistemas de nanopartículas de ouro com quitosano, um polissacárido catiónico, e epigalocatequina galato (EGCG), que contém um elevado poder antioxidante. Outra abordagem consiste no desenvolvimento de nanopartículas de ouro estabilizadas com goma arábica, este polissacárido é muito utilizado na indústria alimentar, e a funcionalização de nanopartículas de ouro com cisteamina, um antioxidante. Posteriormente, os nanosistemas foram conjugados/ carregados com EGCG que exibe efeitos biológicos e farmacológicos como propriedades antioxidantes, propriedades anticancerígenas e anti-inflamatórios.

Partículas de pequenas dimensões foram sintetizadas e otimizadas. Nanosistemas estáveis foram preparados com EGCG, apresentam uma eficiência de 34±8% para as nanoparticulas com EGCG; para as nanopartículas de ouro conjugadas com EGCG sintetizadas com quitosano cerca 60±2%, as partículas de ouro obtidas pelo método Turkevitch e funcionalizadas com cisteamina cerca de 78±1% de EGCG. As partículas de ouro estilizadas com goma arábica adsorveram 14 ± 2% de EGCG

EGCG tem propriedades antioxidantes, por isso, realizou-se uma análise a todos os nanosistemas. Confirmando-se que os mesmos não perderam atividade ao serem conjugados/ carregados com as nanopartículas de ouro.

Estes resultados demonstram que EGCG pode agir como agente redutor, e como estabilizador. A eficiente preparação, conjugação e otimização dos nanosistemas pode ser uma nova abordagem como sistemas de distribuição de agentes.

Palavras-chave: Partículas de ouro, epigalocatequina galato, conjugação, estabilizador, eficiência, antioxidante

Declaration

I declare, under oath, that this work is original and that all non-original contributions were duly referenced with source identification.

_____

09/2016

Table of Contents

List of figures

List of tables

Abbreviations and Symbols

Abbreviations

A	Absorbance
AuNPs	Gold Nanoparticles
C	Concentration
Cys	Cysteamine
Ch	Chitosan
D	Diameter
DI	Deionized water
DLS	Dynamic light scattering
EGCG	Epigallocathechin gallate
GA	Gum ARABIC
h	hour
min	Minutes
nm	nanometers
PBS	Phosphate buffered saline
PdI	Polydispersity index
min	Minutes
mV	miliVolts
T	Absolute temperature value
TEM	Transmissions electron microscopy

Symbols

D_S	Translational diffusion coefficient
$\boldsymbol{\varepsilon}$	Extinction coefficient
ε	Dielectric constant
F	Force of interaction between the tip and the surface of the sample
F(ka)	Henrys function
I_0	Incident light intensity
I	Light intensity that passes through a volume
k	Spring contact of the cantilever
k	Boltzmann's constant
L	Distance through the sample
R_H	Hydrodynamic radius of the scattering particles

T	Transmittance
μ_E	Electrophoretic mobility
ŋ	Viscosity
ζ	Zeta potential

Chapter 1

1. Preface

Cancer is one of the leading causes of morbidity and mortality all over the world. As claimed by the GLOBOCAN series of the International Agency for Research on Cancer, it was concluded that there are 14.1 million new cancer cases, 8.2 million cancer deaths and 32.6 million people living with cancer[1].

Nanoparticle formulation, functionalization and characterization are important advances in biomedicine as promising delivery systems for cancer treatments and diagnosis. Colloidal gold nanoparticles have been the focus of increasing number of research studies. They have been used to deliver of therapeutic chemicals directly to tumour sites, by extending their ability to also act as nanocarriers[2]. They present unique optical and chemical properties that provide them important characteristics used in bionanotechnology to enhance the therapeutic effectiveness of biomolecules. It is fundamental to further development of these nanoparticles for future clinical trials.

This study was conducted to evaluate the efficacy of one of the emerging phytochemicals, epigallocatechin gallate (EGCG) conjugated/ loaded with AuNPs synthesized by different methods. EGCG is an ester of epigallocatechin and gallic acid, and is a type of catechin. Functionalized gold nanoparticles were developed as a strategy for cancer prevention, slowdown or reversion, demonstrating the efficacy of nanoparticulate technology to enhance therapeutic effectiveness[3].

The thesis is organized into five chapters. This chapter, Introduction, presents the purposes and scope of this research. Chapter 2, Background, introduces the state-of-art of drug delivery systems in cancer treatment. In Chapter 3, Material and Methods, the preparation and characterization of the nanosystems are described. In Chapter 4, the stability study of EGCG, the physical characterization and the stability studies of the AuNPs synthetized with EGCG, the conjugation of EGCG with AuNPs synthetized with chitosan, the conjugation of EGCG with AuNPs synthetized by Turkevich method and functionalized with cysteamine, the loaded of EGCG with AuNPs stabilized with Arabic gum. In the Chapter 5, concluding remarks, future work and other applications of AuNPs were presented.

Chapter 2

2.Background

2.1 Introduction

For more than a decade, the majority of nanotechnology-based research has been focused on targeted drug delivery to overcome the limitations of conventional therapies [1,2.] Recently, it was introduced a novel concept of "nanochemoprevention" [3]. The main propose of this concept is based on the minimization of the anticancer drug side-effects. Nanosystems are being developed leading to high bioavailability as well as to activate the drugs *in situ* [4]. In addition, the reactivity of the surface chemistry of nanosystems allows for conjugation of targeting ligands for activate targeted delivery[5].

Several nanosystems such as liposomes, nanocrystals, micelles, metal based nanoparticles, nanoemulsions, quantum dots and polymer nanoparticles have being developed for treatment and diagnosis of various types of cancer[5,7]. Triggered response is one way for drug molecules to be put to use more efficiently, so it is very important to be taken in consideration the biocompatibility, biodegradability and stability[8]. Thus, the ability to adjust the pharmacokinetics and biodistribution of the drug in the body determines the strength of the drug[8]. Moreover the small size of the nanoparticles might improve the take up by cancer cells[9]. However other physicochemical properties such as chemical composition, shape, roughness, hydrophobicity, hydrophilicity and surface charge have influence on biocompatibility and stability of the nanosystems [10.11,12]. Table 2.1 highlights the most important nanoparticle platforms used in nanocarrier preparation for applications as drug delivery system (DDS) [7,13,14].

Therefore, DDS may overcome in an efficacy treatment resulting in a therapy with reduced side effects, decreasing exposure of chemotherapeutics to healthy cells [5]

Table 2.1: Nanosystems for drug delivery systems

Liposomes	Phospolipid
Micelles	Copolymers
Dendrimer	Poly(amidoamine)
Inorganic nanoparticles	Gold nanoparticles (AuNPs); carbon nanotubes; mesoporous silica nanoparticles
Fullerenes	Carbon based nanocarriers
Polymeric nanoparticles	Polysaccharides including chitosan, gum arabic, hyaluronic acid; Polyethyleinemine.

2.2 Design of nanoparticles for anticancer drug delivery

Among various cancer treatments, chemotherapy is a major therapeutic approach. There are several chemotherapeutic agents limitations such as high costs, lack of efficiency, elevated toxicity on healthy proliferating cells causing various side effects including anemia, exhaustion, nausea and hair loss and acquisition of multidrug resistance (MDR) against anticancer drugs [5,15].

Nanometer-size materials are expected to have a revolutionary impact on biology and medicine[16]. They can improve the limitations of the chemotherapy agents[16]. Therefore, nanoparticles loaded with phytochemicals have an important impact on therapeutics facilitating the drug delivery, increasing the efficacy of the drug and improving its circulation and stability. Also, nanoparticles might induce the decrease of toxic side effects in healthy tissues[17].

Carcinogenesis is recognized as a complex and multistep process. It occurs a distinct molecular and cellular modification, resulting in an uncontrolled growth of the tumor cells that involves the gradual conversion of premalignant cells to neoplastic ones with an increase of invasiveness and metastasis potential and new blood vessel formation (Figure 2.1) [3,95].

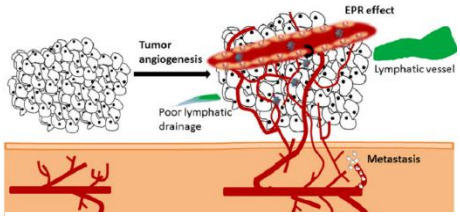

Figure 2.1: Angiogenesis processes[95].

Nanoparticles can increase the drug retention in tumor tissue, due to the enhanced permeability and retention effect, improving the intra-cellular penetration and the target specificity[18].

One major potential mechanism of action for reducing damage caused by disease is antioxidation[8,19]. Actually, phytochemicals, specific marker agents for cancer cells, are being used to modify the drug nanosystems [8]. Phytochemicals have emerged as a potential strategy for an effective chemotherapeutics, because of the high spectrum of biological activity, low cost and minimal side effects[20]. The advantages and disadvantages of phytochemicals are summarized in Table 2.2[21,12, 22,17,19].

Table 2.2: Advantages and disadvantages of phytochemicals.

Phytochemicals advantages
Alterations of cell cycle control, apoptosis evasion, angiogenesis and metastases
Synergize with cytotoxic drugs, increasing their efficacy and lowering the toxic side effects on normal cells
Delay resistance onset
Targeting delivery at site
Antioxidant activity
Phytochemicals disadvantages
Particle aggregation, making physical handling of nanoparticles difficult in liquid and dry forms
Toxicity of materials

The use of phytochemicals can inhibit the carcinogenesis process involved in numerous signaling pathways and biological mechanisms related with cancer development and progression[3,8]. These marks are able due to the possibility of surface functionalization [3].

Several studies demonstrated numerous phytochemicals present in medicinal plants that can induce cytotoxicity against various types of cancerous cells. Table 2.3 presents some of the phytochemicals that have been reported to possess anticancer activity[19,18].

Table 2.3: Phytochemicals clinically tested in cancerous patients.

Phytochemicals	Patients	Intervention	Effect
Green tea	Patients with high-grade prostate intraepithelial neoplasia	600 mg/day green tea catechins, orally, for one year	After 1 year, the incidence of tumor development was 3% and 30% in treated and control men, respectively; quality of life improved[23].
	Patients with histologically confirmed adenocarcinoma of the prostate	Usual tea consumption	The prostate cancer risk declined with increasing frequency, duration and quantity of green tea consumption green tea[24].
	Patients with esophageal cancer	Usual tea consumption	consumption was associated with reduced risk of esophageal cancer[25].
Resveratrol	Patients with colorectal cancer	20-80 mg/day of resveratrol containing grape powder for 14 days	Resveratrol did not inhibit the colon cancer but inhibited the pathway in normal colonic mucosa[26].
Curcumin	Patients with urinary bladder cancer, uterine cervical neoplasm, or intestinal metaplasi	500 mg/day, orally, for 3 months	Histologic improvement in 1 out of 2 patients with bladder cancer, 1 out of 6 patients with intestinal metaplasia and 1 out of 4 patients with uterine cervical neoplasm[27]

2.3 Gold Nanoparticles

Metallic nanoparticles are subject of an effort research as novel vectors for the specific target delivery of therapeutic agents[28]. Colloidal gold nanoparticles (AuNPs) present suitable properties for a controlled drug delivery[29,28]. They have been studied for applications such as cancer treatment, biomedical imaging and diagnosis due to their outstanding compatibility with the human organism, low toxicity and tunable stability, small diameters, and possibility to interact with a variety of peptides, proteins, antibodies and other biomolecules[9,29]. Thus, they exhibit a combination of unique physical, chemical, optical and electronic properties [30].

The main process for nanoparticles development requires chemical functionalization with capping agents that absorb and/or react with the surface of nanoparticles[31]. Because of this, there are a large number of ways to synthesize AuNPs. The most common method of synthesis is the Turkevitch method[7]. It is based on a single-phase reduction of gold tetracholoauric acid by sodium citrate in an aqueous medium. The nanoparticles size produced is around 20 nm. The Brust-Schiffrin method, also very known, uses tetraoctylammonium bromide as the phase transfer reagent and sodium borohydride as reducing agent resulting nanoparticles with a diameter from 1-5 nm [32].

AuNPs present high electron affinity that allow the tendency to adopt the negative oxidation state -I[28]. Furthermore, AuNPs appear with different morphologies such as spheres, cylinders, platelets, tubes [33]. The optical properties of AuNPs are significant conferring them attractive for biological (bio imaging) and technological (photonics) purposes. [30] The interaction of the light with the electrons on the AuNPs surface allow, at a specific wavelength of light, a combined oscillation of electrons on the AuNPs surface cause a phenomenon called surface plasmon resonance, resulting in strong extinction of light (absorption scattering)[34,35].

Currently, it exists several methods for the synthesis of AuNPs using different types of reducing agents with high advantages for humans such as chitosan and epigallocatechin gallate (EGCG). Also, for the stabilization of AuNPs against aggregation, it is being studied stabilizers such as arabic gum and hyaluronic acid. It is an easy process due to the repulsive forces between the nanoparticles and, also, due to their reactive surface [36]. The properties - shape, size and surface chemistry – play an important role on mediating the physiological behaviors of AuNPs such blood circulation[37], targeting [37], distribution[38], translocation[39], metabolism[40], clearance[41] and inflammation in vivo[42]. A report showed that AuNPs (sized of 5, 10, 20, 30, 60, 80, and 100 nm) can interact with multiple proteins in blood including albumin, fibrinogen, globulin, histone, and insulin[40]. By other hand, several studies reported the fast uptake of positive charges at the particle surface by tumor cells compared with negative NPs, which are considered better systems for clinical applications, due to the fact that positively-charged NPs may prefer interact with the extracellular matrix with the opposite charge, which promote cell uptake resulting on immune reactions [40,]

AuNPs can be used for biomedical applications as drug delivery vectors based on covalent reaction, drug encapsulation, electrostatic adsorption and non-covalent conjugation. Consequently, AuNPs can be designed to deliver drugs and imaging agents that otherwise exhibit low solubility and poor pharmacokinetics such as EGCG, curcumin, etc[43,19,8,17].

For biomedical applications, surface-functionalization of AuNPs is fundamental in order to target them to specific disease tissues, to allow them to selectively interact with cells or biological molecules, and to provide long circulation time [44,15]. In order to increase their monodisperse and

individual structure, the surface modification provides enough net charges on the AuNPs, which may produce electrostatic attraction to the oppositely charged functional groups[40].

The functionalization of AuNPS allows to preserve its unique properties such as strong plasmon resonance band, light scattering[41,29]. The functionalization of AuNPs is frequently achieved by thiol ligands, via thiol – gold affinity interactions such as polyethylene glycol (PEG), cysteamine, glutathione [44,45].

Cysteamine is easily attached to the surface of the AuNPs by the Au-S bonds[46]. Several studies reported the anticancer effects to inhibit cancer development and proliferation[47,48]. In fact, cysteamine not only prevent the metaplasia but also the carcinogenesis of mammary tumor and gastric cancers induced chemically and by radiation[47,48]. An *in vitro* study showed that cysteamine inhibits pancreatic cancer cell migration and invasion through direct inhibition[47,48].

The passive targeting of AuNPs coated with PEG occur due to the biocompatibility, and it provides colloidal stability because nanoparticles with PEG brushes on their surfaces repel each other for steric reasons[44]. Another interesting PEG coating aspect noted is the increase of AuNPs hydrophilicity that can enhance its uptake by cancer cells. Thereby hampering efficient drug delivery to tumors by passive targeting nanoparticles[31]. In addition, functionalized AuNPs with PEG layer increase the nanoparticle stability, in *in vivo* and *in vitro* assays[49.] *In vitro* diagnosis, imaging and cancer therapy rely on AuNPs as DDS and on their characteristic properties: chemical stability, high solubility in water, suitable morphology and limited dispersity, high surface-to-volume ratio, non-toxicity in biologic systems and an easy synthesis and functionalization with a plethora of biomolecules (targeting and also silencing moieties) and anticancer drugs[31].

Anticancer drug molecule can attach to the NPs by electrostatic, hydrogen bonds, and hydrogen bonds[16]. The easy surface modification through thiol linkages provides to introduce chemical functionalities in a single step which allows to carry high drug doses. Therefore noncovalent bonding provides a relatively easy mode of conjugation, coupling ligands to the surface of AuNPs increases the stability of AuNPs [30].For effective delivery to cancer cells several studies showed that AuNPs might be a potential vector to avoid RES clearance and enhance endothelial. Results suggested that Doxorubicin (DOX) loaded AuNPs resulted in enhancement of the cytotoxicity when compared with free DOX.[15] Another study suggested AuNPs functionalized with polyamidoamine (PAMAM) dendrimer-folic and/ or fluorescein isothiocyanate (FITC) conjugate for improvement of targeting and imaging on tumor cells [29].

2.4 Polymeric nanoparticles

Biocompatible, non-toxic, low allergenicity and biodegradable polymers have been used to stabilize AuNPs, or to modify its surface for a specific application. Polymeric NPs confer advantages for the drug deliver, such as:

- An increase of the volatile pharmaceutical agents' stability, easily and cheaply fabricated in large quantities by a multitude of methods;
- A significant improvement over traditional oral and intravenous methods of administration in terms of efficiency and effectiveness;
- A higher concentration of pharmaceutical agent delivery to a desired location;
- Easy incorporation into other activities related to drug delivery, such as tissue engineering[50].

The choice of polymer used and the ability to modify drug release allow to polymeric nanoparticles the ability to be ideal candidates for cancer therapy, delivery of vaccines, contraceptives and delivery of targeted antibiotics [50,44].

The enhanced permeability and retention (EPR) effect provides a basis for the selective accumulation of many current high molecular- weight drugs currently in clinical use, such as Arabic gum (GA) and hyaluronic acid (HA)[30]. Polysaccharide-based AuNPs can be prepared by different mechanisms such as covalent crosslinking by chemical interaction, ionic crosslinking by polyanions/polycations with low molecular weight can act as ionic crosslinkers for charged polysaccharides. The most common crosslinker used is tripolyphosphate (TPP). Also, it could be prepared by polymers with opposite charge surface that can form polysaccharide NPs by electrostatic interaction defined as polyelectrolyte complexation and self-assembly of hydrophobically modified polysaccharides by spontaneous formation of micelles by polymeric amphiphiles through intermolecular connection between hydrophobic moieties[51,52,53]

Chitosan (Ch) is a natural polycationic linear polysaccharide derived from partial deacetylation of chitin. Chitosan is composed of β-(1-4)-linked D-glucosamine and N-acetyl-D-glucosamine randomly distributed within the polymer[54]. The main advantage of Ch is his cationic nature due to the fact of the majority of polysaccharides are neutral or negatively charged an acidic environment[55,54]. Thus, these allow to form electrostatic complexes or multilayer structures with other negatively structures with other negatively charged synthetic or natural polymers[55,56]. Another interesting characteristics are the biocompatibility, non-toxicity, low allergenicity and biodegradability properties[56,57]. The degree of deacetylation and the molecular weight affect the biological effects, such as antitumor, antimicrobial, and antioxidant activities. Studies demonstrated that chitosan exhibited antitumor activity in vitro and in vivo models, investigations showed that it was involved in direct killing of tumor cells by inducing apoptosis[54].

Ch has many advantages, including:

- Ability to bind some organic compounds;

- Susceptibility to enzymatic hydrolysis;
- Intrinsic physiological activity combined with nontoxicity and heavy metal ion;
- Reduces toxicity;
- Slow or controlled drug release which improves drug solubility and stability;
- Enhances efficacy [58].

Studies reported the use of chitosan NP composites as drug delivery systems to cancer treatment. An example suggested is the Ch nanospheres loaded by 5-fluorouracil[58]. This stable nanosized chitosan nanoparticles can entrap and deliver drugs in tumor cells[58]. Other study reported the conjugation of hydrophilic group, methoxy poly-(ethylene)glycol p-nitrophenyl carbonate and an hydrophobic group, cholesteryl chloroformate to the free amine groups of chitosan[59]. The results suggested a high nanoparticle accumulation in a tumor induced murine model and, therefore, a considerable anticancer effect. It was shown a good cytotoxicity of paclitaxel loaded folic acid (FA) modified chitosan NPs in tumor cells[60].

Arabic gum (GA) is negatively charged and made up of glycoprotein and polysaccharide and their calcium, magnesium and potassium salts. The principal polysaccharide is arabic acid, a polysaccharide linking a D-galactose (40% of the residues) with branches composed of Larabinose (24%), L-rhamnose (13%) and D-glucuronic acids (21%). Essentially, the proteins are classified as arabinogalactanes, rich in hydroxproline [61]. It is a biocompatible and biodegradable polymer[62]. Some studies demonstrated that GA acted as a stabilizing agent on AuNPs and it exhibited excellent binding affinity towards on prostate and breast cancer cells[16,63]. Other study suggested GA acting as a reducing agent and stabilizing of gold nanoparticles loaded with DOX, showing an enhancement of the toxicity on human glioma cell lines[16].

Hyaluronic acid (HA) is negative charge, and non-sulphated glycosaminoglycan in the extracellular matrix of many soft connective tissues tissues[6465]. It is composed of alternating units of D-glucuronic acid and N-acetyl-D-glucosamine. HA is an important structural component of tissues in all vertebrates[65]. It is biocompatible, biodegradable, bioactive, non-immunogenic and non thrombogenic[66]. Some studies demonstrated that AuNPs coated with HA exhibited better targeted delivery as well as it increased regression activity in HepG2 cells[67].

Targeted delivery nanosystems can penetrate into cancer cell having important roles for detection, diagnosis and therapy of cancer. Studies supported these NPs as a promising drug delivery system to delivery biomolecules/natural products presenting anti-cancer effects[50].

Chapter 3

3.Materials and Methods

3.1 Materials

Epigallocatechin gallate (MW 458.372 g/ mol) was purchased from Taiyo Kagaku. Chitosan 250 kDa (degree of deacetylation > 93%) was purchased from Altakitin (Portugal) Arabic gum (GA, Mw ~ 250,000, viscosity 60 mPa s), sodium hydroxide and tetrachloroauric (III) acid ($HAuCl_4$; 99.99% trace metals basis, 30 wt% in dilute HCl), acetic acid, dimethyl sulfoxide (DMSO), N-Hydroysulfosuccinimide sodium salt (MW 217.13 g/ mol), n-(3-Dimethylaminopropyl)-N'-ethyliarbodiimied hydrochloride (MW 191.70 g/ mol) and tween 80 were purchased from Sigma-Aldrich (Germany). Phosphate buffered saline (PBS: 0.01 M, 0.0027 M KCl, 0.137 M NaCl, pH 7.4) were purchased from Fluka (Germany). Antioxidant assay kit were obtained from Cayman Chemical Company. Dry Biotech Grade Cellulose Ester dialyses membrane (8-10 kD) was purchased from Spectra/Por®. Amicon ultra (3k) was obtained from Merck KGaA. Cysteamine was brought from Selleck Ckem.

3.2 Systems

3.2.1 Synthesis of gold nanoparticles with Epigallocatechin gallate (EGCG)

An aqueous solution of acid chloroauric (10 mM, 1.0 ml) and Epigallocatechin gallate (EGCG) solution (1.0 mM, 5.0 ml) was mixed under gentle stirring with heat. EGCG was dissolved in water. The color of the mixture turned purple–red from pale yellow within a few minutes, the reaction time was stirred for 15 minutes. The resultant solution (EGCG AuNPs) was centrifuged at 11500 rpm during 10 min to remove the unbound EGCG.

3.2.2 Conjugation of EGCG with gold nanoparticles synthetized with chitosan (EGCG + AuChNPs)

An aqueous solution of acid chloroauric (1 mM, 1 ml) was mixed with diluted solution of chitosan (5 ml, 0.32 w/v%). The mixture was heated under magnetic stirring until a red solution was obtained. The reaction time was 30 min.

Posteriorly, AuChNPs were bioconjugate via carbodiimide-mediated cross-linking of EGCG with AuChNPs. To the solution of EGCG (0.27 mM, 1 ml) under magnetic stirring was add EDC (0.34 mM, 0.2ml) and NHSS (0.34 mM, 0.2ml). Then, 2 ml of AuChNPs was added. The reaction was stirred at room temperature for about 1h. The resultant solution was centrifuged at 12000 rpm during 8 min to remove the excess of EGCG.

3.2.3 Conjugation of EGCG with gold nanoparticles functionalized with cysteamine (EGCG + CysAuNPs)

An aqueous solution of acid chloroauric (25 ml water, 17.2 µl $HAuCl_4$) was mixed with a diluted solution of sodium citrate (2.5 ml, 0.03 g). After a reddish color appeared. The reaction time was 10 min under magnetic stirring and heating. AuNPs were funcionalized with cysteamine. The molar ratio AuNPs: cysteamine is 1:1. The solution was stirred for 30 mins at room temperature.

1 ml of 0.27mM EGCG was conjugated to 5 ml of CysAuNPs via EDC/NHSS coupling reaction, under magnetic stirring, at room temperature. After, tween 80 (0.11 g) was added to the nanoparticles, with 15 min of reaction time. The resultant solution was centrifuged at 12000 rpm during 8 mins to remove the unbound EGCG.

3.2.4 Loading EGCG with gold nanoparticles stabilized with arabic gum (EGCG + GA-AuNPs)

An aqueous solution of $HAuCl_4$ (25 ml water + 17.2 µl $HAuCl_4$) was mixed with a diluted solution of sodium citrate (2.5 ml, 0.03 g) and 500 µl of Arabic gum, with heat and under magnetic stirring. After a reddish color appeared, the reaction time was 10 minutes.

EGCG + GA-AuNPs, was prepared by loading the EGCG to GA-AuNPs. 2 ml of GA-AuNPs solution was add to EGCG in powder (1.22 mg). The solution was mixed by 30 min. The stock solution was centrifuged at 13500 rpm during 8 min to remove the excess of EGCG.

3.3 Methods

3.3.1 Dynamic Light Scattering

Dynamic Light Scattering (DLS) is the most popular methods to determine the size of nanoparticles. To use this equipment, it is necessary to know some parameters as the temperature and viscosity of the sample, but the temperature needs to be stable because of the non-arbitrary movements which can affect the diffusion speed and the size of the particles.

DLS measures the light scattered from a laser that passes through a colloidal solution and by analyzing the modulation of the scattered light intensity as a function of time, the hydrodynamic size of particles and particle agglomerates can be determined[68]. DLS is very sensitive to “soft” flexible biological molecules such as polymers, proteins, and antibodies because the can cause significant drag, which can dramatically influence the rate of the particles’s motion under Brownian diffusion[69].

The hydrodynamic diameter of the particles measured is calculated from the translational diffusion coefficient by using the Stokes-Einstein relation[70]:

$$D_s = \frac{kT}{3\pi\eta R_H} \qquad (3.1)$$

where R_H is laser hydrodynamic radius of the scattering particle; D_s is the translational diffusion coefficient which depends on the size of the particle on the surface structure and on the concentration and type of ions in solution; k is the Boltzmann's constant; T is the absolute temperature; η is the viscosity.

The hydrodynamic diameter of the nanoparticle' suspension was analysed by dynamic light scattering (DLS) using a Zetasizer Nano ZS (Malvern Instruments Ltd., Malvern, UK), keeping the samples at 25ºC. Size measurements were performed at a scattering angle of 173º in a 12 mm square polystyrene cuvette (Sarstedt, Germany).

3.3.2 Zeta Potential

The zeta potential (ζ, ZP) consists on electrostatic potential generated by the accumulation of ions at the surface of the colloidal particles giving an indication of the stability of the system [69].

Nanoparticles have a surface charge that attracts a thin layer of ions of opposite charge to the nanoparticle surface[71]. This double layer of ions travels with the nanoparticle as it diffuses throughout the solution, and when the equilibrium is reached the NPs move with a constant velocity[71]. The velocity depends on the viscosity (η), the zeta potential, the dielectric constant (ε) and its denominated electrophoretic mobility to zeta potential (μ_E).

Henry's equation relates electrophoretic mobility to zeta potential:

$$\mu_E = \frac{2\varepsilon.\zeta.f^{ka}}{3\eta} \qquad (3.2)$$

Where is f^{ka} Henrys function and can be 1.5 or 1.0. It is 1.5 when it is a Smoluchowski approximation for an aqueous solution. For small particles with low dielectric constant and in non-aqueous solutions, the Henrys function is 1.0 and it is the called Huckel approximation.

The magnitude of the zeta potential is predictive of the colloidal stability. Nanoparticles with Zeta Potential values greater than +25 mV or less than -25 mV typically have high degrees of stability. Dispersions with a low zeta potential value will eventually aggregate due to Van Der Waal inter-particle attractions[71].

The zeta potential of nanoparticle suspensions and complexes was determined by laser Doppler velocimetry, respectively, using a Zetasizer Nano ZS (Malvern Instrument s Ltd., Malvern, UK), at 25ºC. The zeta potential was obtained by using a disposable capillary cell (DTS 1060, Malvern).

3.3.3 Transmission Electron Microscopy

Transmission electron microscopy (TEM) technique uses powerful electron beams and can provide a great amount of detail at the atomic scale such as information about the size, structure and geometry of samples[69]. The energy of the electrons in the TEM determines the relative

degree of penetration of electrons in a specific sample. Therefore, the image obtained are two-dimensional sections. The samples are prepared for imaging by drying nanoparticles on a copper grid that is coated with a thin layer of carbon[72].

TEM images were acquired using a Jeol JEM-1400, JEOL operated at 60 kV. 5 µL of each sample was placed on carbon formvar-coated grid and let to adsorb for 5 mins. After, the grid was washed to remove the excess.

3.3.4 Absorption Spectroscopy

The concentration of gold nanoparticles was estimated from UV absorbance (A) between 524 - 570 according to the Beer-Lambert law:

$$A = log_{10}\left(I_0 / I\right) = \varepsilon . \mathrm{C} . \mathrm{L} \qquad (3.3)$$

where *I* is the transmitted intensity, I_0 is the intensity of the incident light at a given wavelength, *L* is the distance through the sample and *C* is the concentration of the absorbing specie; ε is a constant known as the molar absorptivity or extinction coefficient, which is a molecular property in a given solvent at a specific temperature and pressure.

UV-Vis absorption spectra of the samples EGCG AuNPs, EGCG + AuChNPs, EGCG + CysAuNPs and EGCG + GA-AuNPs were carried out using a 1 cm quartz cuvette, at room temperature by Shimadzu UV-1700 PharmaSpec spectrophotometer.

3.3.5 ATR-FTIR

Fourier Transform Infrared spectroscopy is a technique used to identify the absorption peaks which correspond to the frequencies of vibrations between the bonds of the atoms making up the material by comparison with known spectra of compounds[73]. This procedure consists in radiation of infrared which is passed Infrared**.** Some of the infrared radiation is absorbed by the sample and some of it is passed through. The resulting spectrum represents the molecular absorption and transmission, creating a molecular fingerprint of the sample[73].

The Infrared region of the electromagnetic spectrum is usually divided into three regions: far-IR (400-20 cm^{-1} wavenumber), which has adjacent rotational energy level changes; mid-IR (400-1400 cm^{-1}), which has correlated to fundamental vibrational level changes, and near-IR (14000 – 4000 cm^{-1}), which causes vibrational and rotational level changes.

The transmittance (T) is:

$$\mathrm{T} = \frac{\mathrm{I}}{\mathrm{I}_0} = \exp[-\alpha \times \beta] \qquad (3.4)$$

where is the intensity of the transmitted radiation by the sample, is intensity of the incident radiation.

The equipment used has a beam source that contains different frequencies of light at once and it measures how much of that beam is absorbed by the sample. The light shines according to configuration of mirrors denominated Michelson interferometer, which allows some wavelengths to pass through and blocks others. The light from the polychromatic infrared source is accumulated and directed to a beam splitter. The best way is the light reflected from the two mirrors back to the beam splitter and 50% of the original light passes into the sample. After that, the light is refocused to the detector. Then, the measured signal (information about the characteristics frequencies and intensities of the spectrum) is digitized and sent to the computer where the Fourier transformation takes place. The raw data is a set of intensities measured for discrete values of retardation, being interpreted and manipulated according to algorithm Fourier Transform.

3.3.6 *In vitro* release studies

Drug release studies of the EGCg were performed to systems EGCg AuNPs, EGCg + AuChNPs, EGCg + CysAuNPs and EGCG + GA-AuNPs. The studies were carried out at 37ºC using a biotech grade cellulose ester dialysis membrane (molecular weight cut off, MWCO: 8–10 kD, purchased from Spectrum Labs Europe BV, Netherlands). The solutions were incubated in 4 ml of DI water and with constant magnetic stirring.

3.3.7 Antioxidant Assay

The cayman's antioxidant assay kit was used to measure the total antioxidant capacity of the systems EGCG AuNPs, EGCG + AuChNPs, EGCG + CysAuNPs and EGCG + GA-AuNPs. The antioxidants in the sample cause suppression of the absorbance at 750 nm to a degree which is proportional to their concentration.

Chapter 4

4.Epigallocatechin gallate (EGCG)

4.1 Introduction

Epigallocatechin gallate is an ester of epigallocatechin and gallic acid and is a type of catechin[43]. EGCG is characterized by the dihydroxyl or trihydroxyl substitutions on the B ring, this ring is responsible of antioxidant reaction, and the *m*-5,7-dihydroxyl substitutions on the ring A[74]. The antioxidant activities presented on EGCG derives from the presence of phenolic groups that are sensitive to oxidation and it can generate quinone[43,75]. The antioxidative activity is further increased by the presence of the trihydroxyl structure in the D ring in EGCG (Figure 4.1)[43,74,43,75]. It is a powerful radical scavenger, protected neurons from the oxidative damage induced by a commonly used pro-oxidant such as *tert*butylhydroperoxide[43,75]. EGCG can reduced the cytotoxicity evoked by H_2O_2 and increased the levels of the enzymes related to the oxidative stress[43,75,76].

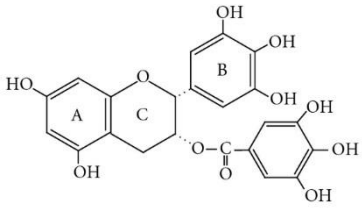

Figure 4.1: Epigallocatechin gallate.

EGCG exhibits the highest protection against DNA scissions, mutations, and in non-enzymatic interception of superoxide anions[44]. Also, some of the benefits of EGCG are[43,77,22]:

- Inhibition effect of cancer-associated stages and on DNA methylation via blocking performance of DNMTs;
- Strong free radical scavenging and antioxidant activities;
- Delaying the promotion of tumor growth by blocking receptors in affected cells. Additionally, EGCG facilitates the direct binding to certain cancer developing carcinogens and it inhibits tumorigenesis in a variety of organs;
- The expression of the multi-drug resistance gene and modulate topoisomerase activity associated with tumor growth;
- Lipopolysaccharide induced nitric oxide production and inducible nitric oxide synthase gene expression in isolated peritoneal macrophages by decreasing the activation of NFκB;
- PDGF-induced apoptosis and cell cycle regulating pathways of vascular smooth muscle cells, resulting in inhibition of tumor growth, metastasis, and angiogenesis;
- Inhibition of malignant cells growth and inducement of apoptosis even in cancerous cell lines resistant to CD95-mediated apoptosis.

Many studies reported the effects of EGCG against cancers of the skin (UV radiation and chemically induced), lung, breast, colon, liver, stomach, prostate, and other sites[78,79,80,2381,82].

Therefore, EGCG displays an array of cellular effects that can disturb all stages of cancer development by up or down regulating multiple key cellular proteins involved in diverse cellular signal transduction pathways: proliferation, differentiation, apoptosis, angiogenesis or metastasis, resulting in a potential beneficial effect[83]. Studies have shown higher toxicity in cancer cells than in their normal counterparts, by the influence of EGCG. *In vitro* studies demonstrated the inhibition of cellular growth and apoptosis in a high number of human cancer cell lines including leukemia, melanoma, breast cancer, lung and colon [83,78,77].

Some of the effects mentioned earlier occurred due to the antiproliferative activity of EGCG on tumor cells through the blockage of growth factor binding to the receptor and the suppression of mitogenic signal transduction[43,84].

EGCG has a large number of advantages over conventional cancer therapies[85,]. Although, it presents a short half-life, low stability and low bioavailability, limiting its use in clinical settings[85,86,87]. In addition, the effective antitumoral concentration in *in vitro studies* is, generally, higher than the levels measured *in vivo*, which restricts its effectiveness[86,87,79]

In order to improve the pharmacokinetic and pharmacodynamics of chemopreventive agents, the synthesis and/or conjugation of phytochemicals on gold nanoparticles might increase its solubility and bioavailability, prolong its circulation time and induce to higher levels of target specificity[86]. Some studies demonstrated the potentials of EGCG conjugated with AuNPs. The inhibition of formation and development of tumors in bladder are reported[20]. In this study it was concluded that AuNPs inhibited the tumor via the mechanism of cell apoptosis[20]. Also, it is being reported the AuNPs study for the treatment of disorders associated with oxidative stress, including neurodegenerative disorders, cardiovascular disease and cancer[64]. In addition, it was demonstrated that EGCG AuNPs as 1.66 times more potent than EGCG for inhibition tumor growth in a murine melanoma mode [84]. Below shows some treatment of cancer with EGCG.

Table 4.1: AuNPs with EGCG to treatment of cancer.

	D (nm)	ZP (mV)	ŋ (%)	Results
AuNPs	-	21 ± 5	-	Inhibition of tumor cell growing by means of cell apoptosis in bladder cancer[20]; Activation of caspase signaling[20]
	25.6 ± 7.26		2.71	Induction of apoptosis in neuroblastoma[74]
	64.7	– 3.36	27	Inhibition of the growth of murine B16F10 melanoma cells[84]

4.2 Results

4.2.1Study of Epigallocatechin gallate (EGCG)

Epigallocatechin gallate (EGCG) is the most prevalent cathechin in green tea extract, to which most of the health benefit of green tea has been attributed.

A calibration curve (Figure 4.2) was performed to determine the concentration of EGCG on AuNPs.

The EGCG stability assay was performed at different pH and temperatures – pH 3 (37ºC), pH 5.3 (37ºC) and pH 7.4 (at 4ºC and 37ºC) and it is visualized on Figure 4.3.

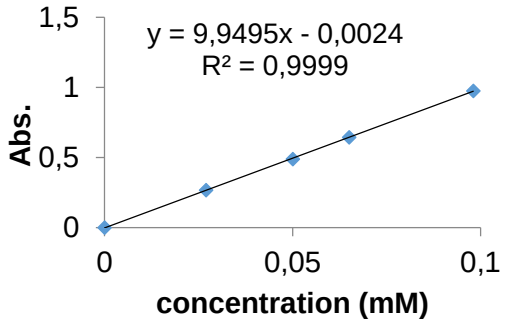

Figure 4.2: Calibration curve of EGCG.

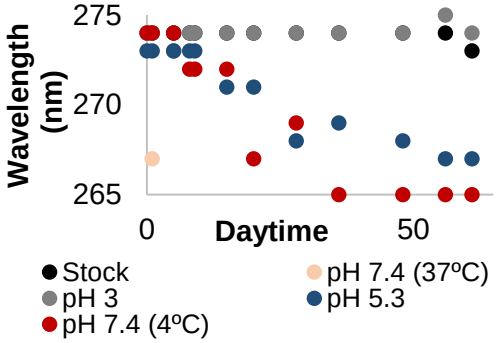

Figure 4.3: Stability study of absorption spectra of EGCG.

It is observed that EGCG is stable at 37º C in acidic conditions, at pH 5.3 (37º C) and pH 7.4 (4ºC), in these conditions the catechin was stable during 62 days. At pH 5.3, a variation of wavelength from 274 nm to 265 nm starting at the 28 day is visualized. At 37º C and pH 7.4, EGCG is not stable.

4.2.3 Antioxidant Assay

The antioxidant activity of EGCG was studied by the antioxidant assay kit in order to confirm its effect, and to be compared with the EGCG conjugation/ loading to AuNPs. A calibration curve of EGCG was performed and presented in Figure 4.5.

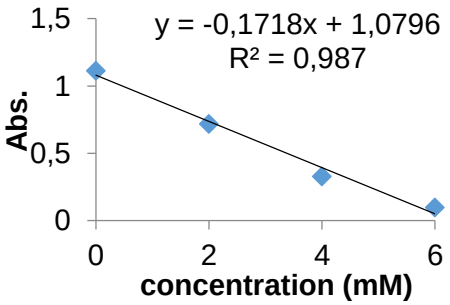

Figure 4.4: Calibration curve of EGCG.

The amount of ABTS (2,2´- Azino -di-3-ethylbenzthiazoline sulphonate] to $ABTS^{+}$ by metmyoglobin was read at 750 nm (Figure 4.4). The assay relies on the ability of EGCG in the sample to inhibit the oxidation of ABTS® (2,2'-azino-di-[3-ethylbenzthiazoline sulphonate]) to ABTS® · + by metmyoglobin.

4.3 Physical characterization of synthesis of AuNPs with EGCG (EGCG AuNPs)

4.3.1 Particles size distribution, surface charge and morphology EGCG AuNPs

AuNPs were synthesized using EGCG as reducing agent. It was studied the formation of the nanoparticles (NPs) and its stabilization when AuNPs were prepared with 0.86 mM, 0.29 mM, 0.0125 mM of EGCG concentration, at different times of reaction. It was concluded that a high period of reaction corresponds to big NPs with low EGCG efficiency. Because of this fact, the synthesis of NPs was performed and optimized using an EGCG concentration of 0.86 mM. The NPs showed more stability and high EGCG efficiency than the others preparations.

Therefore, AuNPs were prepared through the reduction of EGCG by gold salt. The values of hydrodynamic diameter was 104 ± 10 nm and the zeta potential was -34 ± 3 mV that indicates the stability of the suspension of NPs. Also, a low polydispersity index (0.2) of the samples was obtained corresponding to monodisperse NPs.

TEM analyses (Figure 4.6) showed nanoparticles with spherical shape with a size distribution around 30 nm. TEM analysis is not in agreement with DLS measurements. DLS is very sensitive, and measure an ensemble of NPs[69]. So, complementary size characterization by TEM can be useful in cases of these ambiguities because it is not influenced by an agglomerate of NPs[69,68].

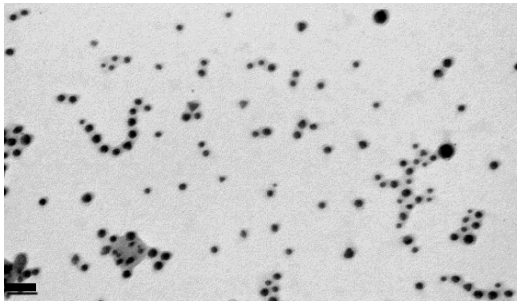

Figure 4.5: TEM image of EGCG AuNPs. The scale bar is 50 nm.

The particles show, in aqueous dispersion, a typical and distinctive surface plasmon resonance confirmed by the peak centered at 530 nm (Figure 4.7).

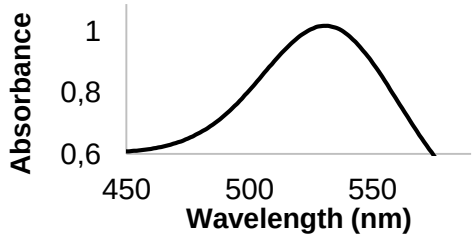

Figure 4.6: Absorption spectra of EGCG AuNPs.

The concentration of AuNPs synthesized using EGCG was 17.5 nM, estimated by the Lambert-Beer Law[88]. EGCG efficiency of the nanosystem was determined by analysis of the nanoparticles supernatant. It was found that EGCG efficiency in AuNPs is 34 ± 8 % that corresponds to 0.53 mM of the catechin in stock solution.

4.3.2 Nanoparticle Stability

The stability of the particle was tested for different pH and temperatures – pH 3 (37ºC), pH 5.3 (37ºC) and pH 7.4 (at 4ºC and 37ºC). The hydrodynamic diameter, the zeta potential and the UV-vis spectra were analyzed and the results are presented in Figure 4.8.

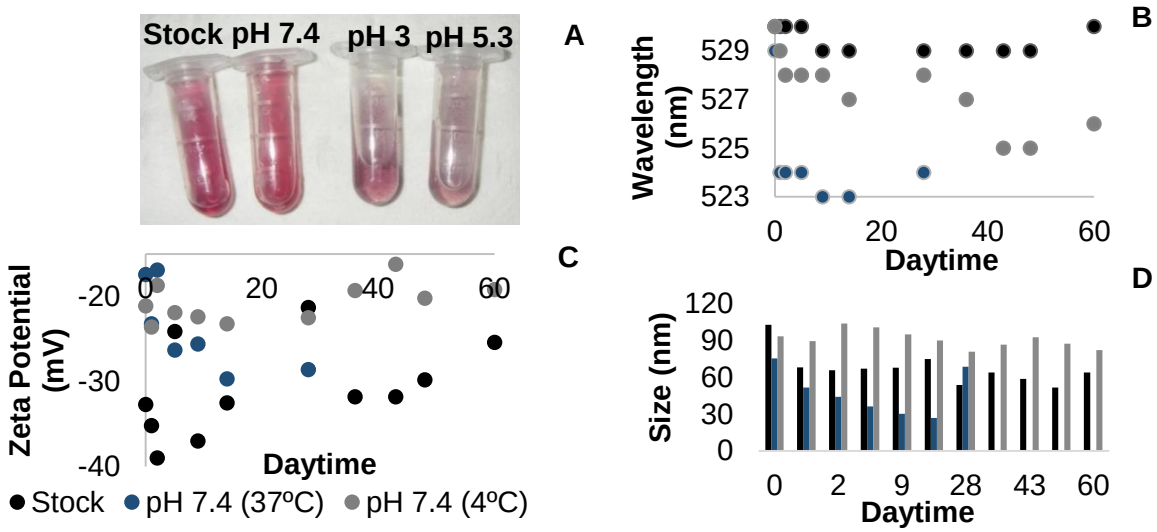

Figure 4.7: A) Visualization of the samples; Stability study assay by **B)** wavelength peak **C)** Zeta potential **D)** Size.

EGCG AuNPs are stable at pH 7.4 (at 4ºC and 37ºC) as noted on Figure 4.8. During the stability study it didn't exist a significant variance on the size at pH 7.4 (4ºC) it maintained around 90 nm, and the stock solution the value of wavelength is constant – 529 nm. However, EGCG AuNPs are not stable at pH 3 (37ºC) and pH 5.3 (37ºC).

4.3.3 Interactions of EGCG with AuNPs

4.3.3.1 ATR-FTIR analysis

The spectra of the sample showed the characteristic peaks at 3361 cm^{-1} for the hydrogen bonded phenols (Figure 4.9 A). At 2991 cm^{-1}, 2903 cm^{-1} and 2855 cm^{-1}, the small peaks correspond to the sp3 C-H stretching in the C ring of the EGCG. It is observed the carboxylic acid bond (C=O) at 1614 cm^{-1} that links the trihydroxybenzoate group and chromane group; at 1575 cm^{-1} and 1456 cm^{-1} the C=C bond in the EGCG aromatic group. At 1408 and 1256 cm^{-1} peaks indicate the C-O stretching of ester functional group and at 1066 cm^{-1} the C-O stretching of phenols. The aromatic C-H bending is observed at 902 cm^{-1}. Figure 4.9 showed the ATR-FTIR analysis of EGCG AuNPs

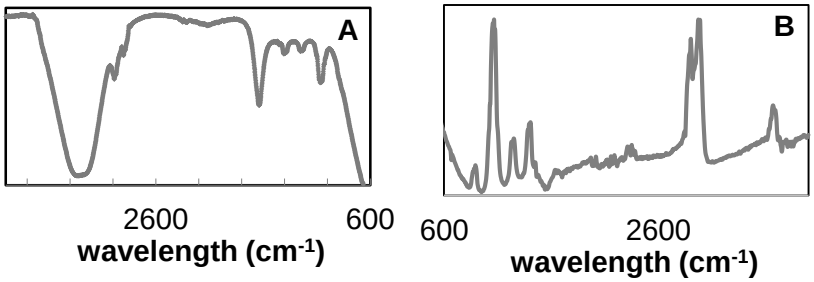

Figure 4.8: FTIR A) EGCG AuNPs spectra B) EGCG AuNPs spectra subtracted to the spectra of the water.

4.3.3.2 Antioxidant Assay

The behavior and interactions of EGCG AuNPs were studied by the antioxidant assay kit in order to confirm the effect of EGCG, and it was obtained 3.0 mM. Based on the result, EGCG AuNPs has the capacity to inhibit the oxidation of ABTS. Therefore, EGCG did not lose its antioxidant capacity when used for the synthesis of AuNPs.

4.3.4 *In vitro* release studies

In vitro release experiment of EGCG AuNPs was investigated using dialysis membranes in DI water, at 37º C.

The result of EGCG AuNPs is depicted on Figure 4.10.

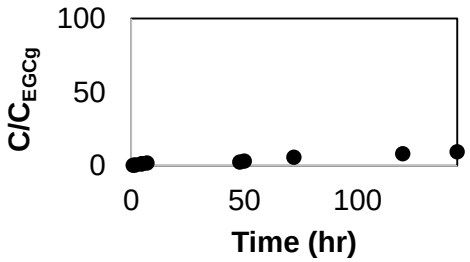

Figure 4.9: Release study of EGCG AuNPs.

The release profile showed that the EGCG release in water is very slow, after seven days only 10% of the EGCG was released. This could be justified by the fact that EGCG acts as a reducing agent in the formation of AuNPs, and might exist a chemical reaction between them decreasing its release.

4.4 Physical characterization of EGCG conjugated with AuChNPs (EGCG + AuChNPs)

4.4.1 Particle size distribution, surface charge and morphology of EGCG + AuChNPs

The electrostatic attractive forces between amino groups in chitosan and metal salt ions ($AuCl_4$) in solution provide an effective driving force in formation and stabilization of these metal nanoparticles[89]. In fact, it was studied the role of Ch as a reducing agent and as stabilizer in the formation of gold nanoparticles. Nanoparticles were prepared with 0.20%, 0.32% and 0.40% of chitosan (w/v%). The results suggested that a high Ch concentration corresponds to large nanoparticles.

The optimal AuChNPs were prepared with Ch concentration of 0.32% w/v. These NPs prepared with 0.32% w/v of Ch showed more electrostatically stability than the others Ch concentrations used.

Cationic chitosan AuNPs were prepared through the reduction of gold salt by Ch. The bioconjugation of chitosan gold nanoparticles with EGCG was developed via carbodiimide-mediated cross-linking.

The size distribution and zeta potential of AuChNPs samples were presented in Table 4.4.

Table 4.2: Hydrodynamic diameter, polydispersity index (PdI) and zeta potential of AuChNPs.

	H_2O		
Parameters[1] / **Sample**	**D(nm)**	**PdI**	**ZP (mV)**
AuChNPs (Stock)	86 ± 16	0.2	22 ± 5
EGCG + AuChNPs (Stock)	125 ± 13	0.3	36 ± 6

[1]D, diameter; ZP, zeta potential

The zeta potential of AuChNPs changed from 22±5.0 mV to 36 ± 6 mV after the conjugation of 0.08 mM of EGCG. However, this result suggests an increase on the stability of the nanoparticles. Also, it is observable different sizes before and after of the conjugation, from 86 nm to 125 nm which means the conjugation increases the size of AuNPs. The high size deviation occurs because of the degree of deacetylation of chitosan that promotes the increase of the PdI (Table 4.4).

TEM analyses, presented in Figure 4.11, showed nanoparticles with spherical shape.

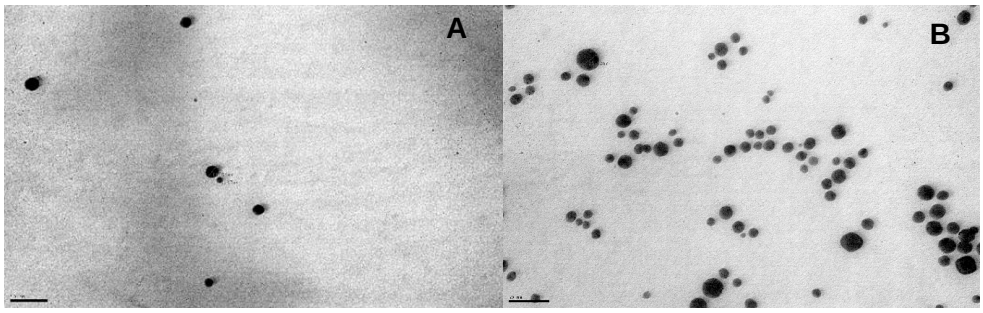

Figure 4.10: TEM image of **A)** AuChNPs **B)** EGCG + AuChNPs. The scale bar of TEM is 50 nm.

In aqueous dispersion, EGCG + AuChNPs showed a typical surface plasmon resonance band centered at 524 nm (Figure 4.12 A).

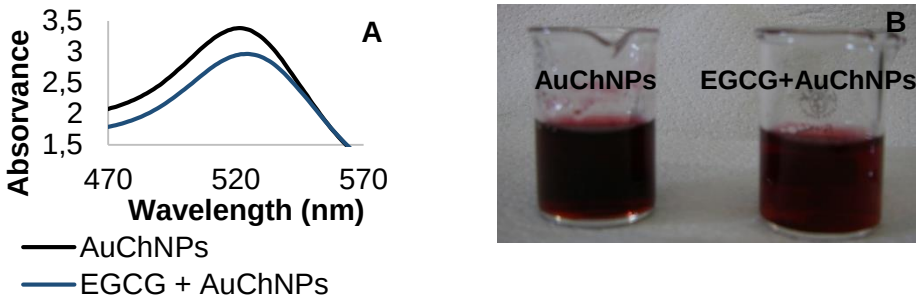

Figure 4.11: A) Absorption spectra of samples; B) AuChNPs and EGCG + AuChNPs image.

The concentration of EGCG + AuChNPs stock solution is 14.5 nM, estimated by Lambert-Beer[88]. The EGCG efficiency of the nanosystem was determined by analysis of the supernatant removed from nanoparticles. It was found that EGCG efficiency on AuChNPs is 60± 2% corresponding to a EGCG concentration of 0.033 mM.

4.4.2 Nanoparticle stability

Figure 4.12 presents the values of the hydrodynamic diameter, zeta potential and the UV-vis spectra of the suspensions prepared. The experiments were performed at different pH and temperatures: pH 3 (37ºC), pH 5.3 (37ºC) and pH 7.4 (at 4ºC and 37ºC).

Before the stability study of the bioconjugation it was made a study stability of AuChNPs. Based in Figure 4.13, AuChNPs are stable at different pH, unless at pH 3. It is visible at pH 5.3 the shift of peak from 524 nm to 544 nm that corroborates with the size that tends to increase, meaning the aggregation of AuChNPs on 9th day (Figure 4.13 B, D).

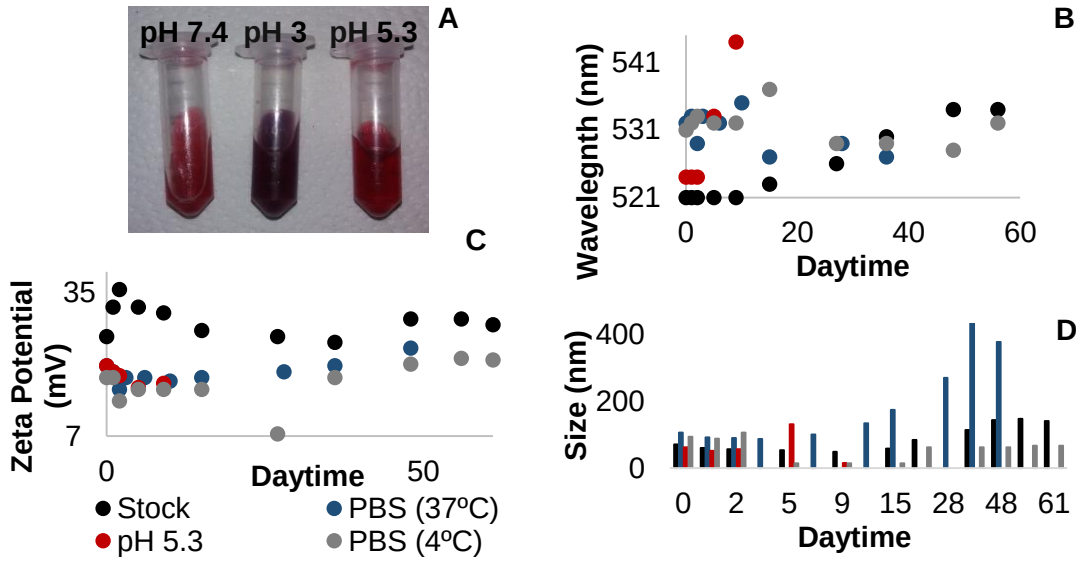

Figure 4.12: Image of the samples; Stability study assay by B) wavelength peak **C)** Zeta Potential **D)** Hydrodynamic diameter of EGCG AuNPs.

The study of bioconjugates stability shows that they are unstable at pH 3 as observable on Figure 4.14 A due its significant change of color from red to grey. At 37ºC and pH 7.4, it is shown significant differences when compared with AuChNPs. These results suggest that in these conditions EGCG promotes the instability of AuChNPs resulting in the aggregation of the nanosystem on the second day, during these days the zeta potential remained at 6 mV (Figure 4.14 B, C, D). On the other hand, at pH 5.3 the NPs are more stable conjugated, existing a significant different on the wavelength from 520 to 531 nm on 8th day (Figure 4.14 B).

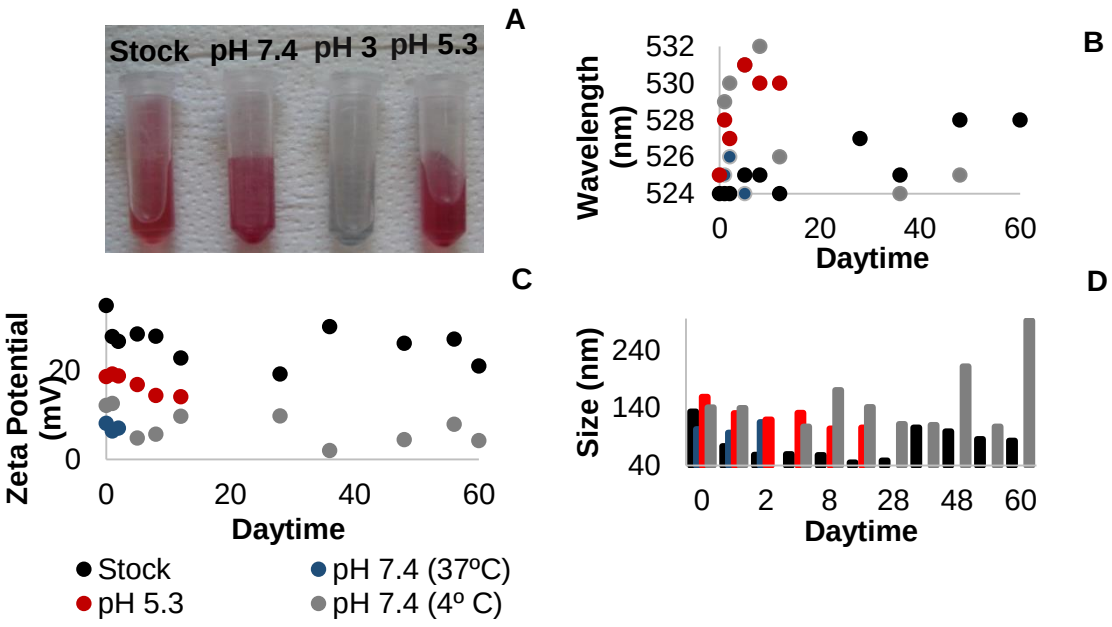

Figure 4.13: A) Samples visualization; Stability study of **B)** Wavelength **C)** Zeta Potential **D)** Size of EGCG + AuChNPs.

4.4.3 Interactions of EGCG + AuChNPs

4.4.3.1 FTIR analyses

Figure 4.15 showed the ATR-FTIR analysis of EGCG AuNPs.

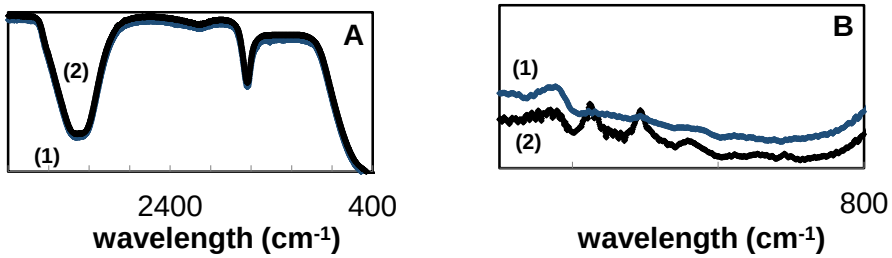

Figure 4.14: FTIR spectra **A)** of (1) AuChNPs (2) EGCG + AuChNPs; **B)** subtracted to the spectra of the water (1) AuChNPs (2) EGCG + AuChNPs.

Two different samples were analyzed by ATR-FTIR spectroscopy (Figure 4.15 A): synthesis of AuNPs with Ch (1) and EGCG loaded AuChNPs (2). The spectra of the sample 1 showed a band at 3335 cm^{-1} (amine N-H symmetric vibration and O-H group); at 2920 cm^{-1} from C-H group and at 1668 cm^{-1} and 1553 cm^{-1} the C-O stretching along with N-H deformation mode (acetylated amine, and to free amine groups). This last band indicates that the chitosan functioned not only as the stabilizer but also as the reducing agent on the synthesis of gold nanoparticles. The CH_3 vibrations are presented at 1421 cm^{-1} and at 1296 cm^{-1}; at 1301 cm^{-1} presented the C-N bond. The spectra of the sample 2 showed a band at 3290 cm^{-1} for amine group. At 1553 cm^{-1} the C-O stretching along with N-H deformation mode disappeared. A chemical modification by EDC/NHSS occurred and it is formed an amide bind covalently from chitosan of AuChNPs and polyphenol EGCG (1661 cm^{-1}) [90].

4.4.3.2 Antioxidant Assay

The antioxidant activity of EGCG conjugated with AuChNPs was studied by the antioxidant assay kit.

Table 4.3: Antioxidant assay of AuChNPs + EGCG.

Sample / Wavelength (nm)	AuChNPs	EGCG + AuChNPs (mM)
750	-	2.5

The results suggested that EGCG + AuChNPs nanosystem has the capacity to inhibit the oxidation of ABTS that means that catechin activity do not change when conjugated with AuChNPs. An interesting aspect about the system AuChNPs is the existence of studies suggest that Ch presents antioxidant capacity[54,91]. In this study, Ch acts as a reducing agent of AuNPs that might induce its antioxidant capacity due to their interactions with AuNPs.

4.4.4 *In vitro* release studies

The *in vitro* release experiment of EGCG + AuChNPs were investigated using dialysis membranes in water at 37º C.

The results of EGCG + AuChNPs are depicted in Figure 4.16.

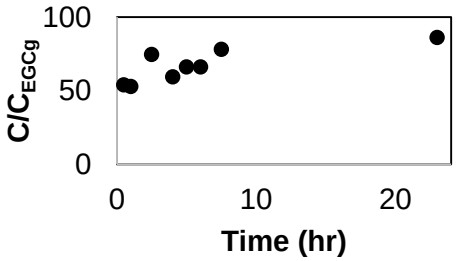

Figure 4.15: Release study of EGCG + AuChNPs.

The EGCG release on AuChNPs is fast. In fact, after 30 min, 54% of EGCG was released. After 7 hours the amount of EGCG released was 99.4%, and in 24 hours occurred the stabilization of EGCG in solution. These finding besides are very important to understand the drug release of the system, and this is an approximate way to explain its transport for the efficient delivery system[92].

4.5 Physical characterization of EGCG conjugated with AuNPs functionalized with cysteamine (EGCG + CysAuNPs)

4.5.1 Particles size distribution, surface charge and morphology of synthesis of EGCG + CysAuNPs

Gold nanoparticles were synthesized by Turkevitch method and funcionalized with cysteamine[7]. It was studied the functionalization of AuNPs with 0.0124 M of cysteamine. Small nanoparticles were obtained.

Different attempts were performed in order to conjugate/load catechin to NPs. EGCG conjugation with AuNPs was experimented via carbodiimide-mediated cross-linking. Also, it was tried the EGCG adsorption to AuNPs surface. Due to aggregation problems, the cysteamine concentration used to funcionalized AuNPs was optimized. The number of moles of cysteamine used is lower than the number of moles of AuNPs. Also, the optimum procedure for preparation of EGCG + CysAuNPs is via carbodiimide-mediated cross-linking.

The size distribution and zeta potential of EGCG + CysAuNPs samples were determined by dynamic light scattering (DLS) and laser Doppler velocimetry, respectively (Figure 4.6).

Table 4.4: Hydrodynamic diameter, polydispersity index (PdI) and Zeta potential of EGCG + CysAuNPs.

	H_2O		
Parameters[1] / **Sample**	**D(nm)**	**PdI**	**ZP (mV)**
AuNPS (Stock)	37 ± 1.4	0.6	-33 ± 2
CysAuNPs	54 ± 9	0.6	-37 ± 3
EGCG + CysAuNPs	110 ± 1	0.2	-23 ± 1

[1]D, diameter; ZP, zeta potential

An interesting aspect visualized on the Table 4.6 is the significant change of size induced by the functionalization with Cys from 37 ± 1.4 nm to 46 ± 0.010 nm, and by the conjugation of EGCG on AuNPs from 46 ± 0.010 nm to 110 ± 0.220 nm. Therefore, the functionalization and conjugation increases the size of NPs. The lower polydispersity index of the final NPs suggests a monodisperse sample. The zeta potential of CysAuNPs changed from -37 ± 3.0 mV to -23 ± 0.2 mV after the 0.08 mM of EGCG conjugation with CysAuNPs. This result might suggests an efficient bioconjugation of the catechin.

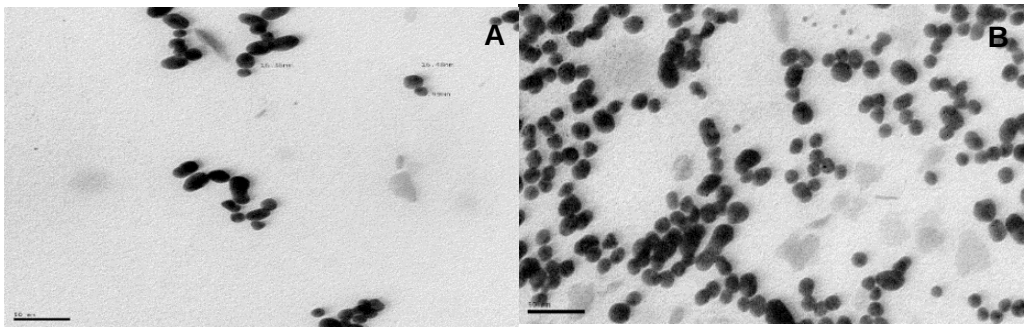

Figure 4.16: TEM image of A) CysAuNPs B) EGCG + CysAuNPs. The scale bar of TEM is 50 nm.

TEM (Figure 4.17) show nanoparticles with spherical and elongated shape with a size distribution around 1 to 15 nm. The analysis of the diameter of the NPs obtained by DLS and by TEM was performed. It is possible to observe that nanoparticles diameters are very different when the techniques are compared[68,69]. TEM method shows NPs morphology and each particle is sized individually, but the samples must be dehydrated and immobilized on a solid support. For DLS, each experiment measures the size of an ensemble of particles, which is prone to errors, is required to estimate the average and distribution of particle sizes[93].

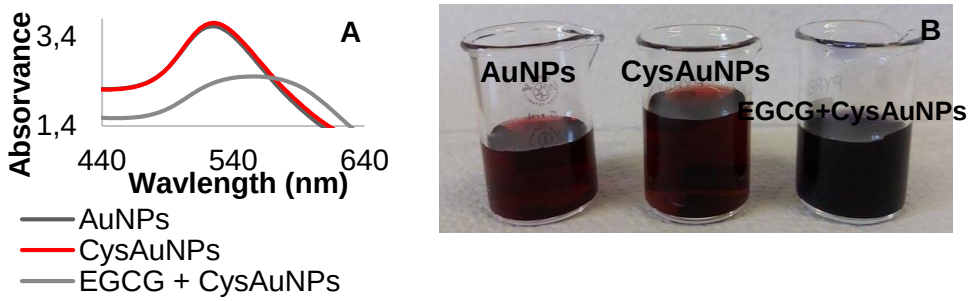

Figure 4.17: A) Absorption spectra of AuNPs, CysAuNPs and EGCg + CysAuNPs **B)** CysAuNPs, and EGCG + CysAuNPs visualization.

The concentration of EGCG + CysAuNPs stock solution, estimated by Lambert-Beer[88], is 10 nM (Figure 4.18). The efficient of the present nanosystems corresponds to 78±1.3% of EGCG on the Cys AuNPs.

4.5.2 Nanoparticle Stability

The NPs stability was measured for pH 3 (37ºC), pH 5.3 (37ºC) and pH 7.4 (at 4ºC and 37ºC). The nanoparticle stability assay showed that EGCG + CysAuNPs is stable at different pH and temperatures (Figure 4.18), only at pH 5.3 (37ºC) is stable during two days having a wavelength value around 533 nm. However, a low zeta potential and high absorption peak were observed (Figure 4.17 B, C). These differences could correspond to functionalization of AuNPs with cystemine. Cysteamine might induce gold nanoparticles aggregation due to the formation of zwitterionic networks involving head-to-head interaction of the deprotonated carboxylate (COO^-) and protonated amine (NH_3^+) groups of one AuNP-bound Cysteamine with the opposite groups of Cys adsorbed on adjacent nanoparticles[94]. Also this is the reason for the significant change of the NPs from red to purple (Figure 4.19 A). Another interesting aspect is at pH 7.4 (37ºC) the wavelength during the 60 days maintained around 528 nm (Figure 4.19 B). Also, at pH 7.4 (4ºC) the zeta potential kept at -7 mV during the study stability (Figure 4.19 C).

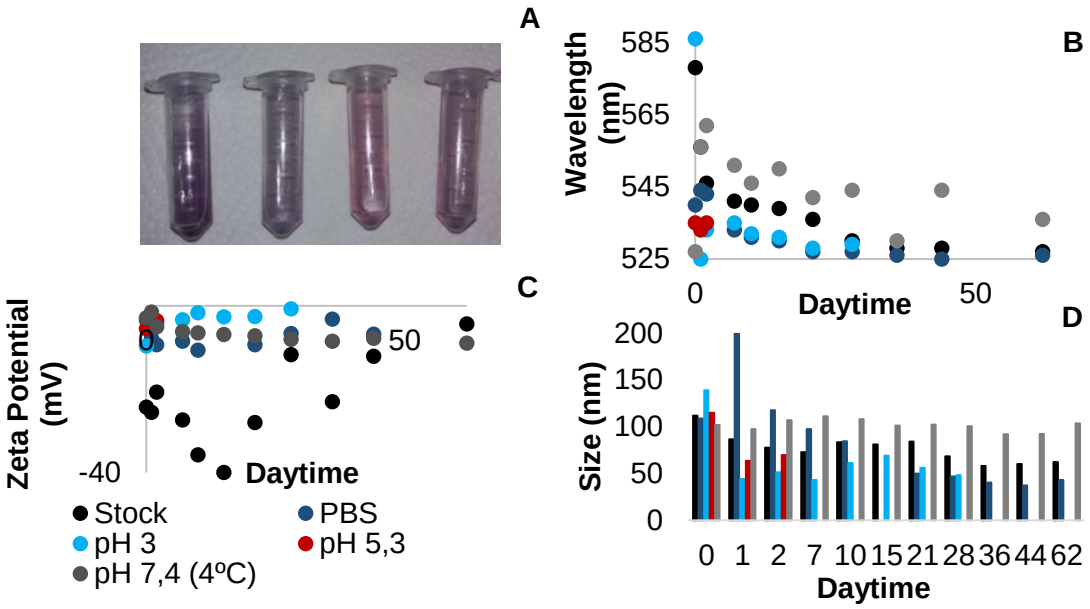

Figure 4. 18: A) Samples image at different pH; Stability study of **B)** Wavelength **C)** Zeta Potential **D)** Size of EGCG + CysAuNPs.

4.5.3 EGCG interactions with CysAuNPs

4.5.3.1 FTIR analyses

ATR-FTIR analysis was made for both nanosystems as depicted in Figure 4.20.

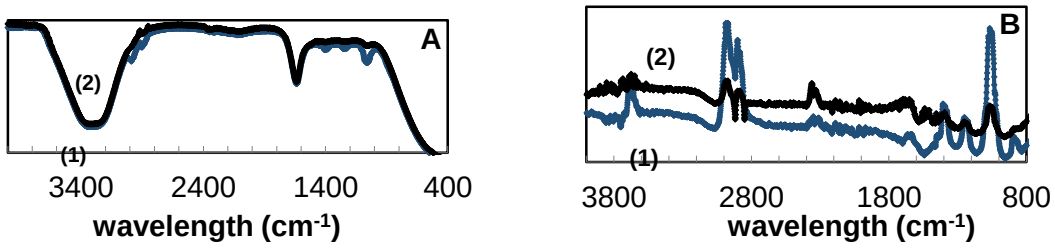

Figure 4.19: FTIR spectra **A)** of (1) CysAuNPs (2) EGCG + CysAuNPs; **B)** subtracted to the water **(1)** CysAuNPs **(2)** EGCG + CysAuNPs.

Two different samples were analyzed by ATR-FTIR spectroscopy (Figure 4.19 A): AuNPs functionalized with cysteamine (1) and EGCG conjugated with AuNPs functionalized with cysteamine (2). The spectra of the sample 1 showed a band at 3653 cm^{-1} and 3671 cm^{-1} the N-H stretch bond of primary amine. An intensive peak at 2988 cm^{-1} indicates C-H of alkanes. 2903 cm^{-1} wavelength corresponds to an C-H stretch of aldehyde. The peak at 1661 cm^{-1} and 2051 cm^{-1} might indicate the salt formed by CSH with HCl ($-NH_3^+$). 1409 cm^{-1} peak corresponds to the strong symmetric vibration of the $\nu C{=}O$; 1245 cm^{-1} band which indicates the stretching vibration of C-N bond.

The spectra of the sample 2 showed the peak at 1542 cm^{-1} the N-H bond from amide linked by alcohol group of polyphenol EGCG and primary amine of the nanoparticles, via EDC/NHSS coupling reaction[90].It is observed the C-H group of aromatic ring at 845 cm^{-1}.

4.5.3.2 Antioxidant Assay

The behavior and interactions of EGCG conjugated with CysAuNPs were studied and presented in Table 4.7

Table 4.5: Antioxidant assay of CysAuNPs and EGCG + CysAuNPs.

Sample / Wavelength (nm)	CysAuNPs	EGCG + CysAuNPs (mM)
750	1.8	3.5

It was confirmed that antioxidant activity of EGCG + CysAuNPs corresponds to a high value determined by the antioxidant kit. Some antioxidant activity was, also, obtained to CysAuNPs nanosystems. This data appears because cysteamine is an antioxidant agent for the treatment of nephropathic cystinosis[47].

4.5.4 *In vitro* release studies

Through dialysis membranes in DI Water at 37º C it was performed an *in vitro* release experiment of EGCG + CysAuNPs.

Figure 4.21 show the result obtained.

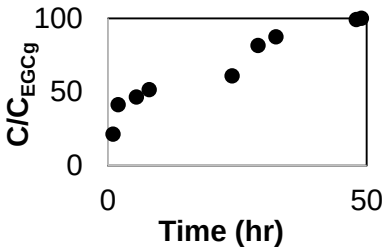

Figure 4.20: Release study of EGCG + CysAuNPs.

Based on the results EGCG was released in water fast, in 2 hours was released 51.4 % and in 48h it was achieved 100%. These findings are particularly important to explain the EGCG + CysAuNPs behavior.

4.6 Physical characterization of EGCG loaded to AuNPs stabilized with Arabic gum (EGCG + GA-AuNPs)

4.6.1 Particles size distribution, surface charge and morphology of EGCG + GA-AuNPs

Some studies were performed with hyaluronic acid (HA) acting as a reducing agent on AuNPs synthesis. Nevertheless, the preparation was no able to achieve because of HA pH (6.7) that is not the same as AuNPs (around 4.8). [95,96]. Other studies were performed: the functionalization of AuNPs with HA or using HA as stabilizer of AuNPs.

However, functionalization of AuNPs with HA promotes higher larger nanoparticles, which is not the propose of the study. By stability tests, it was found that HA is not stable at different pH.

To design AuNPs with HA it will be necessary more research time.

A different approach was performed and a negative polysaccharide was chosen – the arabic gum, GA.

GA is water soluble and it is commercially available as a free-flowing off white-powder. It is a polysaccharide FDA approved. It ca be used for non-food, cosmetic and pharmaceutical[16,61,97]. Besides that, GA provides stability to several nanosystems at different pH[98].

GA was used as stabilizer agent and coating layer of AuNPs[99] (Table 4.8). 33±0.4 nm GA-AuNPs were synthesized and 116±9 nm functionalized GA-AuNPs were obtained. The selected procedure was the use of GA as stabilizer in order to achieve nanoparticles with low diameters.

Table 4.6: Hydrodynamic diameter and Zeta potential of GA-AuNPs.

		H_2O	
Parameters[1] / **Sample**	**Method**	**D(nm)**	**ZP (mV)**
GA-AuNPS (Stock)	**Synthesis**	33 ± 0.4	-31 ± 2
	Functionalization	116 ± 9	-40 ± 5

GA-AuNPs were prepared through the reduction of gold salt by trisodium citrate and using GA as stabilizer (Table 4.9). Then, a physical process – adsorption was chosen to load EGCG to the high reactive GA-AuNPs surface [20,21].

Based on the results from Table 4.9, the final nanosystems present a higher size after the adsorption. The zeta potential of the nanoparticles did not change, significantly, after absorption of EGCG on the NPs surface (from -31±2 mV to -34±2 mV). This values indicates stable colloidal systems.

Table 4.7: Hydrodynamic diameter, polydispersity index (PdI) and Zeta potential of EGCG + GA-AuNPs.

	H_2O		
Sample \ **Parameters**[1]	**D(nm)**	**PdI**	**ZP (mV)**
GA-AuNPS (Stock)	33 ± 0.4	0.57	-31 ± 2
EGCG + GA-AuNPS (Stock)	52 ± 1.4	0.65	-34 ± 2

[1]D, diameter; ZP, zeta potential

From TEM analysis, spherical and triangular nanoparticles are visualized (Figure 4.22).

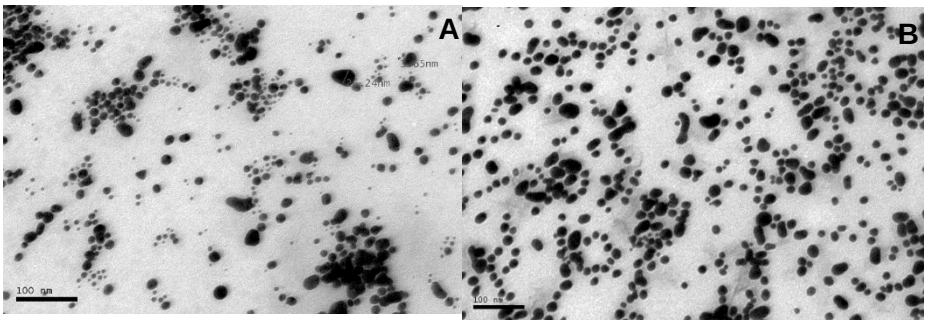

Figure 4.21: TEM image of A) GA-AuNPs; B) EGCG + GA-AuNPs. The scale bar of TEM is 100 nm.

The diameter measured by DLS was larger than TEM size, due to the fact that DLS measure a colloidal solution, and in solution exist more tendency to form an agglomerate of AuNPs. Thus, it was determined the diameter of an agglomerate of GA-AuNPs and EGCG + GA-AuNPs[68]. TEM analyses was required to solve these misunderstandings.

Figure 4.23 B shows a slight difference of red after and before of the conjugation. Also, EGCG + GA-AuNPs the resonance band centered at 526 nm (Figure 4.23 A).

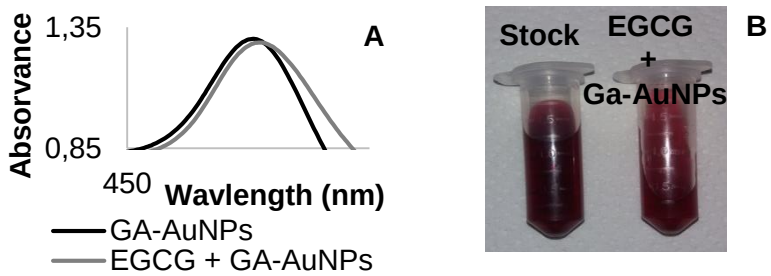

Figure 4.22: A) Absorption spectra of GA-AuNPs and EGCG + GA-AuNPs **B)** GA-AuNPs and EGCG + GA-AuNPs visualization.

The concentration of EGCG + GA-AuNPs stock solution is 11 nM, estimated by Lambert-Beer [88]. The EGCG loading efficiency of the nanosystem was determined by analysis of the nanoparticles supernatant and it was found 14 ± 2% that corresponds to 1.1 mM of EGCG concentration in solution.

4.6.2 Nanoparticle Stability

The particle stability was measured at pH 3 (37ºC), pH 5.3 (37ºC) and pH 7.4 (at 4ºC and 37ºC).

It is possible to observe that GA-AuNPs are stable at different pH and temperatures. In Figure 4.24 A it is observed a significant difference of color from red to purple, and the formation of aggregates at pH 3 on the 20th day and at pH 5.3 on the 28th day. Although, for pH 5.3 the wavelength maintained around 527 nm during twenty days. Additionally, the stock solution showed a size around 30 nm during the study stability. Also, at pH 7.4 (4ºC) it was observed a zeta potential of -20 mV during the 60th days, and a size around 80 nm. However, it occurs a significant change of size on 60th day to 148 nm.

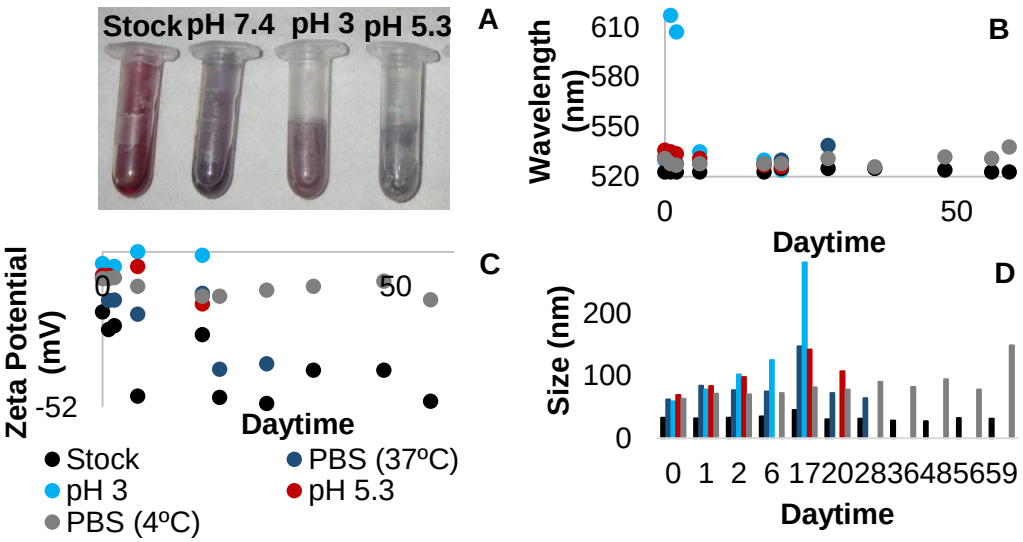

Figure 4.23: A) Samples Image at different pH; Stability study of GA-AuNPs by: **B)** Wavelength **C)** Zeta Potential **D)** Size.

EGCG loaded to GA-AuNPs promotes a significant change on the stability of the NPs as observable in Figure 4.25 C. It is notable a significant modification of color, at pH 3 the grey color indicates the aggregation of NPs on the 1st day. Also, at 5.3 (37ºC) exists a significant change on the wavelength from 538 nm to 560 nm, and on the size from 148 nm to 457 nm which indicates the start of aggregation on the 2nd day. The stock solution presents a constant wavelength – 525 nm - and size, around 50 nm, during the study stability. The same happen at pH 7.4 (4ºC), showing a wavelength at 530 nm and 45 nm of size during 60 days.

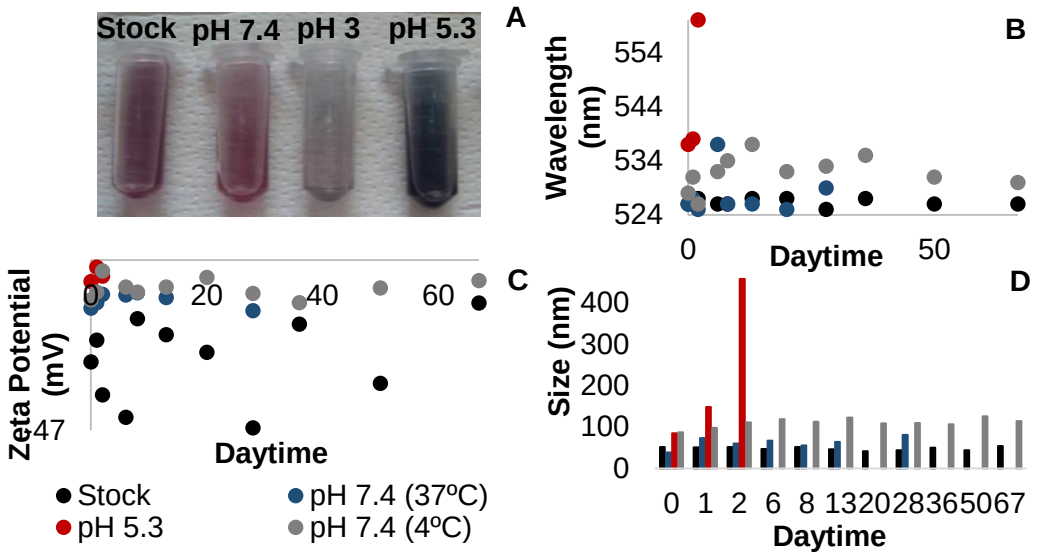

Figure 4.24: A) Visualization of the conjugated samples; Stability study of EGCG + GA-AuNPs by: **B)** Wavelength **C)** Zeta Potential **D)** Size.

4.6.3 EGCG interactions with GA- AuNPs

4.6.3.1 FTIR analyses

In figure 4.26 it is visible the results of EGCG + GA-AuNPs.

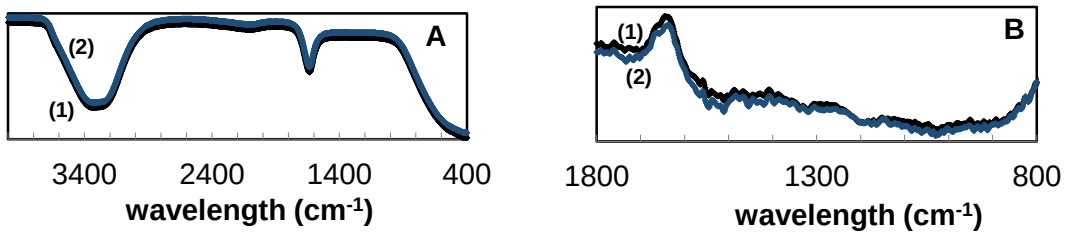

Figure 4.25: FTIR spectra **A)** of (1) GA-AuNPs (2) EGCG + GA-AuNPs; **B)** subtracted to the water (1) GA-AuNPs (2) EGCG + GAAuNPs.

The FTIR spectra of the arabic gum stabilized AuNPs were recorded to identify the functional groups of GA involved in AuNPs preparation. Figure 4.25 show the FTIR spectra of AuNPs stabilized with GA (1) and EGCG loaded AuNPs stabilized with GA (2). The spectra of sample 1 showed a broad band at 3601 cm^{-1} characteristic of the stretching vibrations of the O-H bond. The band at 2859 and 2917 cm^{-1} are attributed to the GA symmetric stretching vibrations of the C-H bond (νC-H of CH_2). The strong vibrational modes located at 1648 and 1700 cm^{-1} could be assigned to the stretching vibrations of the C=O bond of carboxylate group associated with the GA molecules. The two vibrational mode located at 1024 and 1409 cm^{-1}, with relatively low intensity, might be assigned to the stretching vibrations of the C-O bond.

A shift in the pure GA peaks is observed when compared to the sample 1 (data not shown). The shift of the hydroxyl and carbonyl group peaks can interfered and both are involved in the GA-AuNPs synthesis and stabilization.

According to the sample 2 and as it is more easy to visualize in Figure 4.25 B, the presence of EGCG occurred. In fact, at 1664 cm^{-1} it is possible to visualize the C=C aromatic double bond stretching from EGCG. At 1366 cm^{-1} the C-H group presented in the chromane ring of EGCG is observed and, also, at 841 cm^{-1} the C-H group in aromatic ring. The band at 1440 cm^{-1} might be from the aromatic C-C stretching.

4.6.3.2 Antioxidant Assay

Table 4.10 show the antioxidant activity of EGCG loaded with GA-AuNPs studied by the antioxidant assay kit.

Table 4.8: Antioxidant assay of GA-AuNPs and EGCG + GA-AuNPs.

Sample / Wavelength (nm)	GA-AuNPs (mM)	EGCG+ GA-AuNPs (mM)
750	2.1	3.5

The results show that GA-AuNPs has the capacity to inhibit the oxidation of ABTS, antioxidant activity that might be result from arabic gum properties [99,16]. It is also showed a significant increase of the activity on EGCG+ GA-AuNPs nanosystem resulting from catechin loading.

4.6.3.3 *In vitro* release studies

Figure 4.27 depicted *In vitro* release study performed with EGCG + GA-AuNPs using dialysis membranes in water at 37º C.

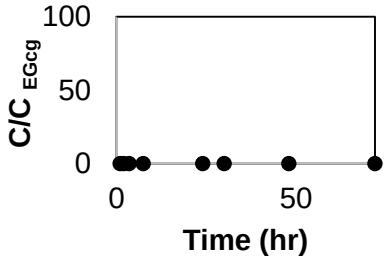

Figure 4.26: Release study of EGCG + GA-AuNPs.

Based on the results, the release study of EGCG + GA-AuNPs is too slow. After, 48h only 0.04% of the EGCG was released. This happened due to the fact that drugs loaded by adsorption may suffer from non-specific release, or other types of interactions[100].

Chapter 5

5.Concluding Remarks

The study analyses different approaches to design of controlled EGCG delivery systems based on AuNPs.

Stable AuNPs were produced and characterized. Although significant differences between the nanosystems were found. Better results were obtained for the nanosystems which were conjugated than those which were loaded or using EGCG as reducing agent. Therefore, using EGCG as a reducing agent decreases the NPs efficiency and promotes a decrease in its antioxidant activity due the chemical reaction that occurs with AuNPs. In addition, considerable differences were observed between physical (adsorption) and chemical (conjugation) processes such as the efficiency and the release of EGCG. Chemical conjugated nanosystems of EGCG + AuChNPs and EGCG + CysAuNPs present a conjugation efficiency of 60±2% and 78±1%, a control release of EGCG 86.2 % and 100% when compared to EGCG absorbed to the NPs surface 14 ± 2%.

Novel EGCG + AuChNPs with positively charged and EGCG + CysAuNPs with negatively charged were successfully prepared, since its charge may influence the cellular effects by a different way. Both nanosystems allow a good controlled release of EGCG and a high antioxidant potential, specially the nanosystem with AuNPs funcionalized with cysteamine. These results suggest that stable polyphenol AuNPs are functional and promising candidates for the treatment of disorders associated with oxidative stress.

More studies need to be performed in the development of nanoparticles for their utility in a wide spectrum of applications such as cancer treatment, cosmetics and food applications.

5.1 Future work

Several successful studies using EGCG in cancer cell lines such as:

- Human colorectal cancer cell lines, HCT-116 and SW-480, studies suggest that has a higher antiproliferative effects [101];
- Human biliary tract cancer, studies demonstrated that EGCG suppresses the growth and invasion potential[82,102];
- Breast cancer cell line MCF-7/BOS, previous studies seem to indicate that suppress the proliferation-stimulating activity of the environmental estrogen[80];
- Colon cancer cells Caco2, HCT116, HT29, SW480, and SW837 studies show that inhibits activation of the epidermal growth factor receptor (EGFR) and human epidermal growth factor receptor-2 and multiple downstream signaling pathways in cancer cell lines[103];
- Leukemic blast cells from AML patients, previous studies seem to suggest that inhibited the proliferation[81].

As future work, I would choose the nanosystems (EGCG + AuChNPs and EGCG + CysAuNPs) that produced the best results to test in cancer cell lines.

According to reported studies, I could choose colorectal cancer lines (HCT-116, SW-480) and human biliary tract cancer lines for *in vitro* cytotoxic studies.

Therefore, safety and therapeutic efficiency of AuNPs are important for their applications in biomedicine. It is necessary to know the factors which influence the cellular effects of gold nanoparticles for the rational design of functional and biocompatible nanocarriers in the future.

5.2 Other applications of the nanosystems developed

Besides cancer treatment, EGCG can be apply to other diseases. A recent study shows that this compound could be used to the treat joint pain, and tissue damage caused by rheumatoid arthritis[104,105]. A previous research seems to indicate that EGCG has an a effect on multiple sclerosis due to the inhibitory effect on inflammation[106]. Another interesting study is the development of drugs with EGCG to combat Down Syndrome, a study demonstrated improvements in executive functions, decision making and brain plasticity [107]. Also, can be used to the treatment of cystinosis[108], to reduce cardiovascular disease, to reduce cholesterol and induce body weight loss[109]. Therefore, EGCG has a high range of applications in biomedicine.

A promising application of EGCG is in cosmetics. The skin is subject to many aggressions increasing the amount of free radicals which can initiate wrinkling, photoaging, elastosis, drying and skin pigmentation. Therefore, due to the fact that EGCG is a powerful antioxidant and could improve skin health.

Bibliography

Bibliography

1. GLOBACAN. International Agency for Research on Cancer. Available at: http://globocan.iarc.fr/Pages/burden_sel.aspx.
2. Singh, M., Harris-Birtill, D. C. C., Markar, S. R., Hanna, G. B. & Elson, D. S. Application of gold nanoparticles for gastrointestinal cancer theranostics: A systematic review. *Nanomedicine Nanotechnology, Biol. Med.* **11,** 1–12 (2015).
3. Manuscript, A. Nanochemoprevention: Sustained Release of Bioactive Food Components for Cancer Prevention. *Nutr Cancer* **62,** 1–6 (2010).
4. Coelho, J. F. *et al.* Drug delivery systems: Advanced technologies potentially applicable in personalized treatments. *EPMA J.* 1–46 (2010). doi:10.1007/s13167-010-0001-x
5. Raavé, R., de Vries, R. B. M., Massuger, L. F., van Kuppevelt, T. H. & Daamen, W. F. Drug delivery systems for ovarian cancer treatment: a systematic review and meta-analysis of animal studies. *PeerJ* **3,** 2–4 (2015).
6. Brown, S. & Khan, D. R. *The Treatment of Breast Cancer Using Liposome Technology*. *Journal of Drug Delivery* **2012,** (2012).
7. Boisselier, E. & Astruc, D. Gold nanoparticles in nanomedicine: preparations, imaging, diagnostics, therapies and toxicity. *Chem. Soc. Rev.* **38,** 2–3 (2009).
8. Rao, P. V. *et al.* Phytochemicals and Biogenic Metallic Nanoparticles as Anticancer Agents. *Oxid. Med. Cell. Longev.* **2016,** 1–4 (2016).
9. Shilo, M. *et al.* The effect of nanoparticle size on the probability to cross the blood-brain barrier: an in-vitro endothelial cell model. *J. Nanobiotechnology* **13,** 1–5 (2015).
10. Papasani, M. R., Wang, G. & Hill, R. A. Gold nanoparticles: The importance of physiological principles to devise strategies for targeted drug delivery. *Nanomedicine Nanotechnology, Biol. Med.* **8,** 1–9 (2012).
11. Zamboni, W. C. *et al. Best practices in cancer nanotechnology: Perspective from NCI nanotechnology alliance*. *Clinical Cancer Research* **18,** (2012).
12. Sonal, S., Prabhakar, V., Aneesh, T. & Sabitha, M. Nanomedicine: Promise Of The Future In Disease Management. *Internet J. Nanotechnol.* **2,** 1–4 (2007).
13. Kumar Khanna, V. Targeted Delivery of Nanomedicines. *ISRN Pharmacol.* **2012,** 2–6 (2012).
14. Ghosh, P., Han, G., De, M., Kim, C. K. & Rotello, V. M. *Gold nanoparticles in delivery applications*. *Advanced Drug Delivery Reviews* **60,** (2008).
15. Madhusudhan, A. *et al.* Efficient pH dependent drug delivery to target cancer cells by gold nanoparticles capped with carboxymethyl chitosan. *Int. J. Mol. Sci.* **15,** 1–2 (2014).
16. Dhar, S., Maheswara Reddy, E., Shiras, A., Pokharkar, V. & Prasad, B. L. V. Natural gum reduced/stabilized gold nanoparticles for drug delivery formulations. *Chem. - A Eur. J.* **14,** 1–6 (2008).

17. Odeh, F., Al-jaber, H. & Khater, D. Nanoflora — How Nanotechnology Enhanced the Use of Active Phytochemicals. *Appl. Nanotechnol. Drug Deliv.* 1–20 (2014). doi:10.5772/58704
18. Yang, C. S., Wang, X., Lu, G. & Picinich, S. C. *Cancer prevention by tea: animal studies, molecular mechanisms and human relevance*. *Nature Reviews Cancer* **9,** (2010).
19. Hosseini, A. G. Cancer therapy with phytochemicals: evidence from clinical studies. *Avicenna J. Phytomedicine* **5,** 1–10 (2015).
20. Hsieh, D. S. *et al.* The treatment of bladder cancer in a mouse model by epigallocatechin-3-gallate-gold nanoparticles. *Biomaterials* **32,** 1–8 (2011).
21. Butt, M. S. & Sultan, M. T. Green tea: nature's defense against malignancies. *Crit. Rev. Food Sci. Nutr.* **49,** 1–9 (2009).
22. Russo, M., Spagnuolo, C., Tedesco, I. & Russo, G. L. *Phytochemicals in cancer prevention and therapy: Truth or dare? Toxins* **2,** (2010).
23. Bettuzzi, S. *et al.* Chemoprevention of human prostate cancer by oral administration of green tea catechins in volunteers with high-grade prostate intraepithelial neoplasia: A preliminary report from a one-year proof-of-principle study. *Cancer Res.* **66,** 1–6 (2006).
24. Jian, L., Xie, L. P., Lee, A. H. & Binns, C. W. Protective effect of green tea against prostate cancer: A case-control study in southeast China. *Int. J. Cancer* **108,** 1–5 (2004).
25. Zheng, P., Zheng, H.-M., Deng, X.-M. & Zhang, Y. Green tea consumption and risk of esophageal cancer: a meta-analysis of epidemiologic studies. *BMC Gastroenterol.* **12,** 1–9 (2012).
26. Nguyen, A. V *et al.* Results of a phase I pilot clinical trial examining the effect of plant-derived resveratrol and grape powder on Wnt pathway target gene expression in colonic mucosa and colon cancer. *Cancer Manag. Res.* **1,** 1–12 (2009).
27. Chang, A., CH, H., JK, L. & TS, S. Phase I clinical trial of curcumin, a chemopreventive agent, in patients with high-risk or pre-malignant lesions. *Anticancer Res.* **21,** 1–6 (2001).
28. Trouiller, A. J., Hebié, S., El Bahhaj, F., Napporn, T. W. & Bertrand, P. Chemistry for oncotheranostic gold nanoparticles. *Eur. J. Med. Chem.* **99,** 1–2 (2015).
29. Tiwari, P. M., Vig, K., Dennis, V. a. & Singh, S. R. Functionalized Gold Nanoparticles and Their Biomedical Applications. *Nanomaterials* **1,** 7–13 (2011).
30. Dreaden, E. C., Austin, L. a, Mackey, M. a & El-Sayed, M. a. Size matters: gold nanoparticles in targeted cancer drug delivery. *Ther. Deliv.* **3,** 1–10 (2012).
31. Silva, J., Fernandes, A. R. & Baptista, P. V. *Application of Nanotechnology in Drug Delivery*. *Application of Nanotechnology in Drug Delivery* (2014). doi:10.5772/57028
32. Arvizo, R. *et al.* Intrinsic therapeutic applications of noble metal nanoparticles: past, present and future. *Chem. Soc. Rev.* **41,** 2–25 (2012).
33. Santhanam, V. Metallic nanoparticles : Building blocks for nanotechnology. 1–3 (2011).
34. Abdelhalim, M. A. K. & M. Mady, M. Physical Properties of Different Gold Nanoparticles:

Ultraviolet-Visible and Fluorescence Measurements. *J. Nanomed. Nanotechnol.* **03,** 1–4 (2012).

35. Parveen, S., Misra, R. & Sahoo, S. K. *Nanoparticles: A boon to drug delivery, therapeutics, diagnostics and imaging*. *Nanomedicine: Nanotechnology, Biology, and Medicine* **8,** (Elsevier Inc., 2012).
36. Sperling, R. a & Parak, W. J. *Surface modification, functionalization and bioconjugation of colloidal inorganic nanoparticles. Philosophical transactions. Series A, Mathematical, physical, and engineering sciences* **368,** (2010).
37. Giuseppe Prencipe, Scott M. Tabakman, Kevin Welsher, Zhuang Liu, Andrew P. Goodwin, L. & Zhang, Joy Henry, and H. D. PEG Branched Polymer for Functionalization of Nanomaterials with Ultralong Blood Circulation. *J Am Chem Soc.* **131,** 1–5 (2010).
38. Luo, L. *et al.* Surface plasmon propelled high-performance CdSe nanoribbons photodetector. **23,** 1–10 (2015).
39. Elbaz, J., Cecconello, A., Fan, Z., Govorov, A. O. & Willner, I. Powering the programmed nanostructure and function of gold nanoparticles with catenated DNA machines. *Nat. Commun.* **4,** 2000 (2013).
40. Wang, P. *et al.* Interaction of gold nanoparticles with proteins and cells. *Sci. Technol. Adv. Mater.* **16,** 1–13 (2015).
41. Zhang, X. D. *et al.* In vivo renal clearance, biodistribution, toxicity of gold nanoclusters. *Biomaterials* **33,** 1–9 (2012).
42. Conde, J. *et al.* In vivo tumor targeting via nanoparticle-mediated therapeutic siRNA coupled to inflammatory response in lung cancer mouse models. *Biomaterials* **34,** 1–9 (2013).
43. Singh, B. N., Shankar, S. & Srivastava, R. K. *Green tea catechin, epigallocatechin-3-gallate (EGCG): Mechanisms, perspectives and clinical applications*. *Biochemical Pharmacology* **82,** (2011).
44. DeLong, R. K. *et al.* Functionalized gold nanoparticles for the binding, stabilization, and delivery of therapeutic DNA, RNA, and other biological macromolecules. *Nanotechnol. Sci. Appl.* **3,** 1–5 (2010).
45. Maus, L., Spatz, J. P. & Fiammengo, R. Quantification and reactivity of functional groups in the Ligand Shell of PEGylated gold nanoparticles via a fluorescence-based assay. *Langmuir* **25,** 1–3 (2009).
46. Mura, S. *et al.* Functionalized gold nanoparticles for the detection of nitrates in water. *Int. J. Environ. Sci. Technol.* **12,** 1–2 (2015).
47. Fujisawa, T. *et al.* Cysteamine suppresses invasion, metastasis and prolongs survival by inhibiting matrix metalloproteinases in a mouse model of human pancreatic cancer. *PLoS One* **7,** 1–9 (2012).

48. Raj K. Puri, Bethesda, M. (US);, Bharat H. Joshi, Bethesda, M. (US); & Benjamin Rubin, Potomac, M. (US). s P u e rv c i n a t l s P u e rv c i n a t l. 1–16 (2014).
49. Manson, J., Kumar, D., Meenan, B. J. & Dixon, D. Polyethylene glycol functionalized gold nanoparticles: The influence of capping density on stability in various media. *Gold Bull* **44,** 1–2 (2011).
50. Muhamad, I. I. & Selvakumaran, S. *Designing Polymeric Nanoparticles for Targeted Drug Delivery System Outline : Nanomedicine* (2014).
51. Patra, C. R., Bhattacharya, R., Mukhopadhyay, D. & Mukherjee, P. Fabrication of gold nanoparticles for targeted therapy in pancreatic cancer. *Adv. Drug Deliv. Rev.* **62,** 1–11 (2010).
52. Glazer, E. S. *et al.* Noninvasive radiofrequency field destruction of pancreatic adenocarcinoma xenografts treated with targeted gold nanoparticles. *Clin. Cancer Res.* **16,** 1–9 (2010).
53. Huang, X., Qian, W., El-Sayed, I. H. & El-Sayed, M. A. The potential use of the enhanced nonlinear properties of gold nanospheres in photothermal cancer therapy. *Lasers Surg. Med.* **39,** 1–7 (2007).
54. Cheung, R. C. F., Ng, T. B., Wong, J. H. & Chan, W. Y. *Chitosan: An update on potential biomedical and pharmaceutical applications*. *Marine Drugs* **13,** (2015).
55. Venkatesan, J. & Kim, S. K. Chitosan composites for bone tissue engineering - An overview. *Mar. Drugs* **8,** 1–10 (2010).
56. Boyles, M. S. P. *et al.* Chitosan functionalisation of gold nanoparticles encourages particle uptake and induces cytotoxicity and pro-inflammatory conditions in phagocytic cells, as well as enhancing particle interactions with serum components. *J. Nanobiotechnology* **13,** 1–17 (2015).
57. Kushwaha Swatantra, K. S., Rai Awani, K. & Satyawan, S. Chitosan: A platform for targeted drug delivery. *Int. J. PharmTech Res.* **2,** 2271–2282 (2010).
58. Elgadir, M. A. *et al. Impact of chitosan composites and chitosan nanoparticle composites on various drug delivery systems: A review*. *Journal of Food and Drug Analysis* **23,** (Elsevier Ltd, 2015).
59. Liu, Z., Jiao, Y., Wang, Y., Zhou, C. & Zhang, Z. Polysaccharides-based nanoparticles as drug delivery systems. *ELSEVIER* **60,** 1–10 (2008).
60. Boddohi, S., Moore, N., Johnson, P. A. & Kipper, M. J. Polysaccharide-based polyelectrolyte complex nanoparticles from chitosan, heparin, and hyaluronan. *Biomacromolecules* **10,** 1–8 (2009).
61. Dauqan, E. & Abdullah, A. Utilization of gum Arabic for industries and human health. *Am. J. Appl. Sci.* **10,** 1–4 (2013).
62. Avadi, M. R. *et al.* Ex Vivo Evaluation of Insulin Nanoparticles Using Chitosan and Arabic

Gum. *ISRN Pharm.* **2011,** 1–2 (2011).

63. Parida, U. K., Biswal, S. K., Nayak, P. L. & Bindhani, B. K. Gold Nano Particles for Biomedical Applications. *World J. Nano Sci. Technol.* **2,** 1–5 (2013).
64. Mero, A. & Campisi, M. *Hyaluronic acid bioconjugates for the delivery of bioactive molecules*. *Polymers* **6,** (2014).
65. Xu, X., Jha, A, Harrington, DA., Farach-Carson, M. *Hyaluronic Acid - Based Hydrogel: from a Natural Polysaccharide to Complex Networks*. *Soft Matter* **8,** (2012).
66. Highley, C. B., Prestwich, G. D. & Burdick, J. A. Recent advances in hyaluronic acid hydrogels for biomedical applications. *ELSEVIER* **40,** 1–2 (2016).
67. Kumar, C. S., Raja, M. D., Sundar, D. S., Gover Antoniraj, M. & Ruckmani, K. Hyaluronic acid co-functionalized gold nanoparticle complex for the targeted delivery of metformin in the treatment of liver cancer (HepG2 cells). *ELSEVIER* **128,** 1–11 (2015).
68. Nanocomposix. NANOCOMPOSIX'S GUIDE TO DYNAMIC LIGHT SCATTERING MEASUREMENT AND ANALYSIS. 1–3 (2015).
69. Dobrovolskaia, M. A. *et al.* Interaction of colloidal gold nanoparticles with human blood: effects on particle size and analysis of plasma protein binding profiles. *Nanomedicine Nanotechnology, Biol. Med.* **5,** 1–11 (2009).
70. Malvern Instruments. Dynamic Light Scattering: An Introduction in 30 Minutes. *Http://Www.Malvern.Com/En/Products/Technology/Dynamic-Light-Scattering/* 1–2 (2000).
71. Nanocomposix. Zeta Potential Analysis of Nanoparticles. *Nanocomposix Publications* 1–6 (2012).
72. Lazar, S., Botton, G. a, Wu, M., Tichelaar, F. D. & Zandbergen, H. W. TRANSMISSION ELECTRON MICROSCOPY ANALYSIS OF NANOPARTICLES. **1.1,** 2–3 (2012).
73. Ganzoury, M. A., Allam, N. K., Nicolet, T. & All, C. Introduction to Fourier Transform Infrared Spectrometry. *Renew. Sustain. Energy Rev.* **50,** 1–8 (2015).
74. Sanna, V. *et al.* Single-step green synthesis and characterization of gold-conjugated polyphenol nanoparticles with antioxidant and biological activities. *Int. J. Nanomedicine* **9,** 1–12 (2014).
75. Weinreb, O., Amit, T., Mandel, S. & Youdim, M. B. H. Neuroprotective molecular mechanisms of (-)-epigallocatechin-3-gallate: A reflective outcome of its antioxidant, iron chelating and neuritogenic properties. *Genes Nutr.* **4,** 283–296 (2009).
76. Nune, S. K. *et al.* Green nanotechnology from tea: phytochemicals in tea as building blocks for production of biocompatible gold nanoparticles. *J. Mater. Chem.* **19,** 2912 (2009).
77. Hoffman, R. EGCG : Potent extract of green tea. *Intelligent Medicine* 1–8 (2013). Available at: http://drhoffman.com/article/egcg-potent-extract-of-green-tea-2/.
78. Khan, N., Afaq, F., Saleem, M., Ahmad, N. & Mukhtar, H. *Targeting multiple signaling pathways by green tea polyphenol (-)-epigallocatechin-3-gallate*. *Cancer Research* **66,**

(2006).

79. Lu, Y.-P. *et al.* Topical applications of caffeine or (-)-epigallocatechin gallate (EGCG) inhibit carcinogenesis and selectively increase apoptosis in UVB-induced skin tumors in mice. *Proc. Natl. Acad. Sci. U. S. A.* **99,** 1–6 (2002).
80. Baker, K. M. & Bauer, A. C. Green Tea Catechin, EGCG, Suppresses PCB 102-Induced Proliferation in Estrogen-Sensitive Breast Cancer Cells. *Int. J. Breast Cancer* **2015,** 1–5 (2015).
81. Asano, Y. *et al.* Effect of (-)-epigallocatechin gallate on leukemic blast cells from patients with acute myeloblastic leukemia. *ELSEVIER* **60,** 1–7 (1997).
82. Takada, M. *et al.* Inhibitory effect of epigallocatechin-3-gallate on growth and invasion in human biliary tract carcinoma cells. *World J. Surg.* **26,** 1–3 (2002).
83. Imtiaz A. Siddiqui, Vaqar M. Adhami, Nihal Ahmad, and H. M. *Nanochemoprevention: Sustained Release of Bioactive Food Components for Cancer Prevention*. *Nutr Cancer* **62,** (2010).
84. Chen, C. C. *et al.* Improving anticancer efficacy of (-)-epigallocatechin-3-gallate gold nanoparticles in murine B16F10 melanoma cells. *Drug Des. Devel. Ther.* **8,** 1–14 (2014).
85. Ramkumar Ponnuraj1*, Janakiraman K1, Sivaraman Gopalakrishnan2, Senthilnathan K2, M. & V2, S. P. FORMULATION AND CHARACTERIZATION OF EPIGALLOCATECHIN GALLATE NANOPARTICLES. *Indo Am. J. Pharm. Res.* **3,** 1–10 (2013).
86. Leu, J. G. *et al.* The effects of gold nanoparticles in wound healing with antioxidant epigallocatechin gallate and α-lipoic acid. *ELSEVIER* **8,** 1–7 (2012).
87. Rahmani, A., Al Shabrmi, F. M., Allemailem, K. S., Aly, S. M. & Khan, M. A. *Implications of Green Tea and Its Constituents in the Prevention of Cancer via the Modulation of Cell Signalling Pathway*. *BioMed research international* **2015,** (2015).
88. Na. Ultraviolet -Visible Spectroscopy (UV). *Rsc* 68 (2014).
89. Huang, H. & Yang, X. Synthesis of chitosan-stabilized gold nanoparticles in the absence/presence of tripolyphosphate. *Biomacromolecules* **5,** 1–4 (2004).
90. Hu, Q. & Luo, Y. *Polyphenol-Chitosan Conjugates: Synthesis, Characterization, and Applications*. *Carbohydrate Polymers* (Elsevier Ltd., 2016). doi:10.1016/j.carbpol.2016.05.109
91. Yen, M. T., Yang, J. H. & Mau, J. L. Antioxidant properties of chitosan from crab shells. *Carbohydr. Polym.* **74,** 1–3 (2008).
92. Joseph, M. M. & Sreelekha, T. T. *Gold nanoparticles - synthesis and applications in cancer management*. *Recent Patents on Materials Science* **7,** (2014).
93. Ito, T., Sun, L., Bevan, M. A. & Crooks, R. M. *Comparison of nanoparticle size and electrophoretic mobility measurements using a carbon-nanotube-based coulter counter, dynamic light scattering, transmission electron microscopy, and phase analysis light*

scattering. *Langmuir* **20,** (2004).

94. Acres, R. G., Feyer, V., Tsud, N., Carlino, E. & Prince, K. C. Mechanisms of aggregation of cysteine functionalized gold nanoparticles. *J. Phys. Chem. C* **118,** 1–2 (2014).
95. Gatej, I., Popa, M. & Rinaudo, M. Role of the pH on hyaluronan behavior in aqueous solution. *Biomacromolecules* **6,** 1–7 (2004).
96. Johns, M. R., Goh, L. T. & Oeggerli, A. *Effect of pH, agitation and aeration on hyaluronic acid production by Streptococcus zooepidemicus*. *Biotechnology Letters* **16,** (1994).
97. Nasir, O. *Renal and extrarenal effects of gum arabic (Acacia senegal) - What can be learned from animal experiments? Kidney and Blood Pressure Research* **37,** (2013).
98. Cotching, B., Simms, R., Kerse, G. & Limited, R. F. C. the Stability of Express Gibberelic Acid in Combination With Liquid Urea. 4–6
99. Djajadisastra, J., Sutriyo, Purnamasari, P. & Pujiyanto, A. Antioxidant activity of gold nanoparticles using gum arabic as a stabilizing agent. *Int. J. Pharm. Pharm. Sci.* **6,** 1–3 (2014).
100. Voliani, V., Italiano, I., Nifos, R., National, I. & Ricci, F. Smart Delivery and Controlled Drug Release with Gold Nanoparticles : New Frontiers in Nanomedicine. (2012). doi:10.2174/1877913111202010034
101. Du, G. J. *et al.* Epigallocatechin gallate (EGCG) is the most effective cancer chemopreventive polyphenol in green tea. *Nutrients* **4,** 1–12 (2012).
102. Senggunprai, L., Kukongviriyapan, V., Prawan, A. & Kukongviriyapan, U. Quercetin and EGCG exhibit chemopreventive effects in cholangiocarcinoma cells via suppression of JAK/STAT signaling pathway. *Phyther. Res.* **28,** 1–7 (2014).
103. Shimizu, M. *et al.* (-) -Epigallocatechin Gallate and Polyphenon E Inhibit Growth and Activation of the Epidermal Growth Factor Receptor and Human Epidermal Growth Factor Receptor-2 Signaling Pathways in Human Colon Cancer Cells. *Cancer Ther. Preclin.* **11,** 1–5 (2005).
104. Marino, A. *et al.* Role of natural antioxidants and potential use of bergamot in treating rheumatoid arthritis. *PharmaNutrition* **3,** 1–5 (2015).
105. Shen, C. L. *et al.* Dietary polyphenols and mechanisms of osteoarthritis. *J. Nutr. Biochem.* **23,** 1367–1377 (2012).
106. A, J. L. *et al.* Polyphenon E, non-futile at neuroprotection in multiple sclerosis but unpredictably hepatotoxic: Phase I single group and phase II randomized placebo-controlled studies. *Ufmg* 898 Available at: http://www.bibliotecadigital.ufmg.br/dspace/bitstream/handle/1843/BUOS-8VVNRK/disserta__o_vers_o_final.pdf?sequence=2.
107. Torre, M. D. e R. de La. Estudo pioneiro encontrou composto que melhora as capacidades intelectuais dos portadores da doença. Available at:

http://visao.sapo.pt/actualidade/sociedade/2016-06-08-Cha-verde-pode-ajudar-pessoas-com-sindroma-de-Down.

108. Cherqui, S. Cysteamine therapy: a treatment for cystinosis, not a cure. *Kidney Int.* **81,** 1–3 (2012).

109. Nor Qhairul Izzreen, M. N. & Mohd Fadzelly, A. B. Phytochemicals and antioxidant properties of different parts of Camellia sinensis leaves from Sabah Tea plantation in Sabah, Malaysia. *Int. Food Res. J.* **20,** 1–4 (2013).